Title: Engineering transposon-associated TnpB-ωRNA system for efficient gene editing and disease treatment in mouse

Authors:

Zhifang Li[1†], Ruochen Guo[1,6†], Xiaozhi Sun[1,2†],Guoling Li[5†], Yuanhua Liu[6], Xiaona Huo[1,2], Rongrong Yang[1,2], Zhuang Shao[1], Hainan Zhang[4], Weihong Zhang[4], Xiaoyin Zhang[1,2], Shuangyu Ma[7], Yinan Yao[6], Xinyu Liu[6], Hui Yang[3,4,6], Chunyi Hu[5*], Yingsi Zhou[4*], Chunlong Xu[1,2,3*]

Affiliations:

1. Lingang Laboratory, Shanghai, China.
2. School of Life Sciences and Technology, ShanghaiTech University, Shanghai, China
3. Shanghai Center for Brain Science and Brain-Inspired Technology, Shanghai, China.
4. HuidaGene Therapeutics Inc., Shanghai, China.
5. Department of Biological Sciences, National University of Singapore, Singapore
6. Institute of Neuroscience, State Key Laboratory of Neuroscience, Key Laboratory of Primate Neurobiology, CAS Center for Excellence in Brain Science and Intelligence Technology, Shanghai Institutes for Biological Sciences, Chinese Academy of Sciences, Shanghai, China.
7. Department of Histoembryology, Genetics and Development Biology, Shanghai Key Laboratory of Reproductive Medicine, Shanghai JiaoTong University School of Medicine, Shanghai, China.

†These authors contributed equally to this work.

***Correspondences:** hu_dbs@nus.edu.sg (C.H.), yingsizhou@huidagene.com (Y.Z.), xucl@lglab.ac.cn (C.X.)

Abstract:

Transposon-associated ribonucleoprotein TnpB is known to be the ancestry endonuclease of diverse Cas12 effector proteins from type-V CRISPR system. Given its small size (409 aa), it is of interest to examine whether engineered TnpB could be used for efficient mammalian genome editing. Here, we showed that the gene editing activity of native TnpB in mouse embryos was already higher than previously identified small-sized Cas12f1. Further stepwise engineering of noncoding RNA (ωRNA or reRNA) component of TnpB significantly elevated the nuclease activity of TnpB. Notably, an optimized TnpB-ωRNA system could be efficiently delivered *in vivo* with single adeno-associated virus (AAV) and prevented the disease phenotype in a tyrosinaemia mouse model. Thus, the engineered miniature TnpB system represents a new addition to the current genome editing toolbox, with the unique feature of the smallest effector size that facilitate efficient AAV delivery for editing of cells and tissues.

Main Text:

Introduction

The TnpB proteins represent a family of transposon-associated RNA-guided endonucleases. Recent biochemical studies[1,2] revealed that TnpB proteins are ancestry predecessors of Cas12 effector proteins in the type-V CRISPR system, and a 247-nucleotides (nt) noncoding RNA (termed ωRNA or reRNA) derived from the right end of transposon element is the required component for TnpB to recognize and cleave target DNA. The size of TnpB proteins, with ~400 amino acid (aa) residues, is much smaller than their evolutionary progeny Cas12 proteins (mostly ~1000 aa). Furthermore, in vitro studies[1,2] demonstrated that TnpB exhibited double-strand DNA cleavage activity guided by ωRNA. Therefore, there is potential for the use of this TnpB system in genome editing and therapeutic applications.

Gene editing using Cas9 or Cas12 systems has been widely used in animal models and recently applied in clinical trials. At present, AAV is the most commonly used delivery system and shown to be safe in gene therapy[3]. However, the maximal cargo size of AAV was limited to be 4.7 kilobase (kb) pairs, hindering efficient in vivo delivery of the large Cas9 or Cas12 protein via single AAV injection. This size problem is exacerbated in the use of base and prime editors comprising Cas9 (or Cas12) and fusion enzymes. Recent identification of compact CRISPR effector proteins Cas12f1 (~500 aa)[4] and Cas13 (~700 aa)[5,6] represent potential solutions. However, the gene editing efficiency of Cas12f1 was relatively low[7-11], whereas Cas13 exhibited collateral RNA cleavage activity with uncertain safety profile[12,13].

In the present study, we demonstrated that genome editing activity of TnpB was markedly higher than that of Cas12f1 in cultured cells and mouse embryos. To further optimize the TnpB system, we engineered TnpB-associated ωRNA in a stepwise manner to identify the optimal ωRNA variant with the shortest sequence length and elevated gene editing activity. Importantly, we showed that the optimized TnpB-ωRNA system could be effectively delivered *in vivo* via a single AAV injection in tyrosinaemia model mice, leading to the prevention of disease phenotype. Thus, we have shown the applicability of the engineered hypercompact TnpB for genome editing *in vivo*.

Results

TnpB exhibited gene editing activity higher than Cas12f1

Previous study has shown the endonuclease activity of several Cas12f1 orthologs from type V-U CRISPR family that have small sizes. As the ancestry enzyme of Cas12 proteins, TnpB (~400 aa) represents the smallest programmable nuclease among common single effector Cas proteins, including SpCas9, LbCas12a, Un1Cas12f1, and IscB (**Fig. 1a**). However, the mammalian genome editing potential of TnpB remained to be fully characterized. Thus, we

selected several genomic loci to evaluate the editing activity of TnpB (from *Deinococcus radiodurans,* ISDra2) in mouse embryos. First, we in vitro transcribed ωRNA that targets the mouse *Tyr* gene (**Fig. 1b**), and inject ωRNA together with TnpB mRNA into mouse embryos. The injected embryos were then transferred into surrogate female mice to generate gene-modified offspring. Since *Tyr* gene encodes the black coat color of C57/B6 mice, we estimated the efficiency of TnpB-induced gene disrupton by directly examining the coat color change in TnpB-injected mice. We found that TnpB treatment completely converted black coat color into albino white in all newborn mice (**Fig. 1c**). In contrast, similar embryo injection of Un1Cas12f1 together with sgRNA targeting the *Tyr* gene did not change the black coat color in the newborn mice (**Fig. 1c**), suggesting a much lower *Tyr* gene disruption efficiency of Un1Cas12f1 than that of TnpB. Further deep-sequencing for *Tyr* gene showed that 20% and 90% of indel mutations were induced by Un1Cas12f1 and TnpB, respectively (**Fig. 1b**). Although Cas12f1 and TnpB have different requirements for target adjacent motif (TAM, also known as PAM) that recognizes the target sequence, we have chosen the targeted sequence in *Tyr* gene to have 17-bp overlap (among 20 bp) for both enzymes (**Fig. 1b**). Thus, the higher editing efficiency of TnpB as compared to Cas12f1 was largely due to its endonuclease activity.

To further evaluate the gene editing activity of TnpB, we chose six additional loci in the mouse *Dmd* gene (**Fig. 1d, Supplementary Fig. 1**) for targeting in mouse embryos, by injecting ωRNA targeting these loci with TnpB mRNA. As shown by deep-sequencing results, TnpB exhibited an average of 90% editing efficiency for all six targeted loci in the *Dmd* gene (**Fig. 1d, Supplementary Fig. 1**). Furthermore, the gene editing outcome was verified by immunostaining of dystrophin protein encoded by *Dmd* gene that is specifically expressed in muscle tissues. In contrast to wildtype mice, TnpB-treated mice showed undetectable dystrophin expression in heart, Diaphragm (DI) and Tibialis anterior (TA) muscles (**Fig. 1e, Supplementary Fig. 2**), suggesting the

complete disruption of *Dmd* gene by TnpB and ωRNA injection. Finally, these immunostaining results were confirmed by Western blotting of dystrophin protein of various muscle tissues (**Fig. 1f**). Consequently, rotarod and grip strength assessment of TnpB-treated DMD mice found functional dysfunction of muscle (**Supplementary Fig. 3**). Thus, our finding indicated more robust gene editing activity of TnpB than that of Un1Cas12f1 in mammalian tissues.

Engineered TnpB-associated ωRNA with elevated editing efficiency

Cognate ωRNA scaffold associated with TnpB is 247 nt, much longer than sgRNA scaffold for most single effector Cas proteins. Previous findings reported that the sgRNA engineering could improve the performance of gene editing enzymes[14]. We thereby hypothesized that ωRNA truncation and optimization might be helpful for enhancing TnpB activity in mammalian cells. To this end, we predicted the secondary structure of ωRNA and formulated a stepwise strategy to truncate ωRNA (**Fig. 2a**). Based on the stem loops in predicted structure, we divided ωRNA into six segments, named as S1 to S6 for the truncation experiment (**Fig. 2b**). To facilitate screen of ωRNA variants, we designed a gene editing reporter with TnpB target DNA placed within a split and frameshifted GFP gene which could only be repaired after disruption of TnpB target sequence to express GFP (**Fig. 2a**). We tested the reporter with cognate ωRNA to prove the conditional activation of GFP after treatment of TnpB guided by ωRNA targeting frameshift mutation in GFP gene (**Fig. 2a**). At first, we deleted S1 to S6 one by one and run the reporter assay. It showed that only deletion of S4 and S6 ablated the activity of TnpB (**Fig. 2c**), suggesting the dispensable role of S1, S2, S3 and S5 for normal ωRNA function. Furthermore, sequence deletion of S1 slightly increase TnpB activity (**Fig. 2c**).

To interrogate combined deletion effect of S1 to S6, we added S2 to S5 deletion in the S1 deletion variant of ωRNA to conduct reporter assay. It found that simultaneous deletion of S1, S2, and S3 in ωRNA-v1 not only supported the

normal function of TnpB but also significantly increased the gene editing efficiency (**Fig. 2d**). These results implied that the ωRNA sequence from S4 to S6 dictated the enzymatic activity of TnpB. Secondary structure of ωRNA after combined truncation of S1, S2 and S3 showed typical stem loop conformations with three distinguishable and consecutive stem loop (SL) domains, termed as SL1, SL2 and SL3(**Fig. 2e**). To further determine the effect of these three SL domains on TnpB activity, we iteratively remove SL1, SL2 and SL3 for reporter test. In addition, we also generated two other ωRNA variants with partial deletion of SL2 subdomain or substitution of G:U with G:C pairs (**Fig. 2e**). We found that SL1, SL2 and SL3 are necessary for the normal function of TnpB since deletion variants lack of any single SL fully blocked the reporter activation (**Fig. 2f**). However, partial replacement of SL3 subdomain with 5'-GAAA-3' loop sequence actually enhance the TnpB activity (**Fig. 2f**). G:C substitution for G:U pair exhibited no additive effect on the performance of TnpB (**Fig. 2f**). Based on these results, we finally identified an optimal ωRNA variant ωRNA-v2 or ωRNA* that improved TnpB performance. Predicted secondary structure of ωRNA* presented with three compact stem loop domains in contrast to loose organization of cognate ωRNA structure (**Fig. 2g**).

Characterization of endogenous gene editing and off-target activity for TnpB-ωRNA system

To verify the reporter assay results for ωRNA*, we selected 14 endogenous genomic loci for further evaluation of gene editing performance in HEK293T (**Fig. 3a**). Among 14 human loci tested, 10 individual target sites showed significant increase of TnpB gene editing efficiency with ωRNA* compared with original ωRNA (**Fig. 3b**). Summary analysis of 14 loci also found significant improvement for TnpB using ωRNA* (**Fig. 3c**). To investigate broad improvement effect of ωRNA* in mammalian cells, we further performed the gene editing in mouse N2a cells targeting four disease relevant genes, including *Klkb1*, *Tyr*, *Hpd* and *Pcsk9*. It found that all genomic sites exhibited

significantly increased gene editing efficiency for ωRNA* compared to original ωRNA (**Supplementary Fig. 4**). Quantitative analysis revealed two fold increase of gene editing efficiency in N2a for ωRNA* versus original ωRNA (**Supplementary Fig. 4**). In particular, ωRNA* even supported TnpB editing of some loci that are barely edited using cognate ωRNA (**Supplementary Fig. 4**). Therefore, we demosntrated the enhanced TnpB activity in mammalian cells via the identification of ωRNA* after stepwise engineering.

To examine the off-target effect of TnpB, we carried out prediction of potential off-target genomic loci with Cas-OFFinder[15] for off-target analysis when designing ωRNA against a target site in Hpd gene (**Fig. 3d**). For the top 10 predicted off-target sites, no gene editing events was detected for Hpd-targeting TnpB-ωRNA (**Fig. 3d**). Furthermore, we also performed genome-wide off-target analysis by PEM-seq[16] to identify potential tranlocation between on-target and off-target loci. Our PEM-seq results showed that there is no induction of translocation events related to gene editing of Hpd gene by TnpB-ωRNA treatment (**Fig. 3e**).

Prevention of fatal liver disease with in vivo delivery of TnpB-ωRNA via single AAV

Given the hypercompact size of TnpB, it would greatly facilitate in vivo delivery via single AAV for gene editing therapy. To demonstrate the potential of TnpB in disease intervention, we chose the *Hpd* as therapeutic target for gene editing therapy of type I hereditary tyrosinaemia (HTI) in $Fah^{-/-}$ mouse model. Adult $Fah^{-/-}$ was administrated with AAV-TnpB or AAV-TnpB-ωRNA (**Fig. 4a**) and kept without NTBC drug, an HPD inhibitor. We observed that AAV-TnpB-ωRNA treated $Fah^{-/-}$ mice was still alive after 75 days without NTBC but all untreated mice died at about 65 days(**Fig. 4b**). Furthermore, $Fah^{-/-}$ mice subject to AAV-TnpB-ωRNA treatment gained body weight after experiencing a short period of weight loss (**Fig. 4c**). Contrarily, untreated mice exhibited rapid weight loss until

death (**Fig. 4c**). Histological analysis found massive liver fibrosis in untreated mice whereas dramatically reduced fibrotic pathology in treated mice (**Fig. 4d**).

Furthermore, we also analyzed the HPD expression in treated versus untreated mice. It showed the remarkable decrease of HPD positive liver region in AAV-TnpB-ωRNA treated mice (**Supplementary Fig. 5a, b**).To investigate the in vivo gene editing outcomes, we collected liver tissue from both treated and untreated mice. We only found 70% indel rate in AAV-TnpB-ωRNA treated mice but no editing events in non-treated animals (**Supplementary Fig. 5c, d**). Consistently, liver metabolic functions were significantly ameliorated after AAV-TnpB-ωRNA treatment as indicated by the blood biochemical profiling results of alanine aminotransferase (ALT), aspartate aminotransferase (AST), total bilirubin and tyrosine (**Supplementary Fig. 6**). Therefore, our results showed the proof-of-concept for applying TnpB in disease control via single AAV delivery in vivo.

Discussion

Diverse CRISPR-Cas systems evolved from immune battle between microbe and mobile genetic elements (MGE), providing us abundant resources for the identification of gene editing enzymes[17]. In the past years, various single effector Cas proteins including Cas9[18], Cas12[19] and Cas13[20] were found to deploy DNA or RNA editing activity in different organisms for both research and therapeutic purpose[21]. Recently, TnpB-like proteins, including IscB and TnpB associated with microbe transposon element, were identified to be active ancestry endonuclease for Cas9 and Cas12[1,2]. Given the hypercompact size of TnpB and IscB, they are excellent candidates for developing miniature gene editing tools that would facilitate in vivo delivery via AAV. To this end, our present study demonstrated the potential of TnpB for robust genome editing in both cultured cells and animal tissues. Although Kim et al. recently reported engineering base editor from a 557-aa ‘TnpB’[22], both Siksnys and Doudna

group lately demonstrated that 'TnpB' used by Kim et al. study should be actually annotated as Cas12f1 that works as dimer unlike monomer TnpB[23,24]. Thus, our work was the first study to extensively show the rational optimization of TnpB to achieve excellent in vitro and in vivo performance for gene editing. Furthermore, we also showed the effectiveness of TnpB based gene editing therapy to prevent fatal genetic disease in mouse model of tyrosineamia via in vivo single AAV delivery of TnpB and ωRNA. Interestingly, we performed stepwise truncation of cognate ωRNA to generate a ωRNA variant with short sequence and high efficiency. Our study represent a good start point to optimize TnpB or even IscB for more broad and convenient use in research and therapeutic scenario.

Endonuclease activity of TnpB was only shown with limited data in 2021 by Karvelis et al study[1]. Extensive characterization of TnpB activity in mammalian cell and tissue were currently needed. Our finding corroborated the results from Karvelis et al study, revealing unexpected higher activity for TnpB than Cas12f1 without further engineering. Moreover, we showed that deletion of 5'-end and partial internal sequence in ωRNA could enhance the gene editing performance of TnpB both in vitro and in vivo. Intriguingly, such deletion strategy was supported by two latest structural studies[25,26] of TnpB-ωRNA-DNA ternary complex published last month, suggesting the potential useful applicability of our ωRNA engineering strategy for more TnpB-like systems. In addition, the TnpB structure could accelerate the rational engineering of such compact enzyme with more demanding properties such as relaxed limitation of target-adjacent motif (TAM), enhanced editing activity and specificity etc.

Gene editing therapy was partly impeded by the limited AAV cargo capacity of only ~4.7 kb considering the fact that common Cas9, Cas12 and their derived base or prime editors have protein size beyond 1000 aa[3,27]. TnpB with less than 500 aa are highly desired gene editing enzymes for AAV delivery in vivo. Our

results with TnpB in treating fatal tyrosineamia in mice signify the advantage of reducing gene editing cargo size despite the modest modification efficiency for Hpd target gene after TnpB-ωRNA optimization. Besides, compact TnpB size could permit using sophisticated regulatory sequences for switchable gene editing and reducing the AAV administration dose for high expression to enable safe therapeutic applications. Furthermore, our optimized ωRNA* variant with less than 100 nt would also be easy for synthesizing chemically modified ωRNA, which is very useful for ribonucleoprotein(RNP)-based gene editing applications.

Overall, our study demonstrated improved gene editing activity of TnpB via ωRNA engineering in cultured cells and showed its disease prevention ability in animal models, indicating the potential of hypercompact TnpB-ωRNA system as effective miniature gene editing modality for more AAV-based disease treatment in animal models and even human patients.

References

1 Karvelis, T. *et al.* Transposon-associated TnpB is a programmable RNA-guided DNA endonuclease. *Nature* **599**, 692-696, doi:10.1038/s41586-021-04058-1 (2021).

2 Altae-Tran, H. *et al.* The widespread IS200/IS605 transposon family encodes diverse programmable RNA-guided endonucleases. *Science (New York, N.Y.)* **374**, 57-65, doi:10.1126/science.abj6856 (2021).

3 Wang, D., Zhang, F. & Gao, G. CRISPR-Based Therapeutic Genome Editing: Strategies and In Vivo Delivery by AAV Vectors. *Cell* **181**, 136-150, doi:10.1016/j.cell.2020.03.023 (2020).

4 Harrington, L. B. *et al.* Programmed DNA destruction by miniature CRISPR-Cas14 enzymes. *Science (New York, N.Y.)* **362**, 839-842, doi:10.1126/science.aav4294 (2018).

5 Xu, C. *et al.* Programmable RNA editing with compact CRISPR-Cas13 systems from uncultivated microbes. *Nature methods* **18**, 499-506, doi:10.1038/s41592-021-01124-4 (2021).

6 Kannan, S. *et al.* Compact RNA editors with small Cas13 proteins. *Nature biotechnology* **40**, 194-197, doi:10.1038/s41587-021-01030-2 (2022).

7 Kim, D. Y. *et al.* Efficient CRISPR editing with a hypercompact Cas12f1 and engineered guide RNAs delivered by adeno-associated virus. *Nature biotechnology* **40**, 94-102, doi:10.1038/s41587-021-01009-z (2022).

8 Kong, X. *et al.* Engineered CRISPR-OsCas12f1 and RhCas12f1 with robust activities and expanded target range for genome editing. *Nature communications* **14**, 2046, doi:10.1038/s41467-023-37829-7 (2023).

9 Bigelyte, G. *et al.* Miniature type V-F CRISPR-Cas nucleases enable targeted DNA modification in cells. *Nature communications* **12**, 6191, doi:10.1038/s41467-021-26469-4 (2021).

10 Wu, Z. *et al.* Programmed genome editing by a miniature CRISPR-Cas12f nuclease. *Nature chemical biology* **17**, 1132-1138, doi:10.1038/s41589-021-00868-6 (2021).

11 Xu, X. *et al.* Engineered miniature CRISPR-Cas system for mammalian genome regulation and editing. *Molecular cell* **81**, 4333-4345.e4334, doi:10.1016/j.molcel.2021.08.008 (2021).

12 Tong, H. *et al.* High-fidelity Cas13 variants for targeted RNA degradation with minimal collateral effects. *Nature biotechnology* **41**, 108-119, doi:10.1038/s41587-022-01419-7 (2023).

13 Li, Y. *et al.* The collateral activity of RfxCas13d can induce lethality in a RfxCas13d knock-in mouse model. *Genome biology* **24**, 20, doi:10.1186/s13059-023-02860-w (2023).

14 Nowak, C. M., Lawson, S., Zerez, M. & Bleris, L. Guide RNA engineering for versatile Cas9 functionality. *Nucleic acids research* **44**, 9555-9564, doi:10.1093/nar/gkw908 (2016).

15 Bae, S., Park, J. & Kim, J. S. Cas-OFFinder: a fast and versatile algorithm that searches for potential off-target sites of Cas9 RNA-guided endonucleases. *Bioinformatics (Oxford, England)* **30**, 1473-1475, doi:10.1093/bioinformatics/btu048 (2014).

16 Yin, J. *et al.* Optimizing genome editing strategy by primer-extension-mediated sequencing. *Cell Discov* **5**, 18, doi:10.1038/s41421-019-0088-8 (2019).

17 Makarova, K. S. *et al.* Evolutionary classification of CRISPR-Cas systems: a burst of class 2 and derived variants. *Nature reviews. Microbiology* **18**, 67-83, doi:10.1038/s41579-019-0299-x (2020).

18 Cong, L. *et al.* Multiplex genome engineering using CRISPR/Cas systems. *Science (New York, N.Y.)* **339**, 819-823, doi:10.1126/science.1231143 (2013).

19 Zetsche, B. *et al.* Cpf1 is a single RNA-guided endonuclease of a class 2 CRISPR-Cas system. *Cell* **163**, 759-771, doi:10.1016/j.cell.2015.09.038 (2015).

20 Abudayyeh, O. O. *et al.* RNA targeting with CRISPR-Cas13. *Nature* **550**, 280-284, doi:10.1038/nature24049 (2017).

21 Wang, J. Y. & Doudna, J. A. CRISPR technology: A decade of genome editing is only the beginning. *Science (New York, N.Y.)* **379**, eadd8643, doi:10.1126/science.add8643 (2023).

22 Kim, D. Y. *et al.* Hypercompact adenine base editors based on transposase B guided by engineered RNA. *Nature chemical biology* **18**, 1005-1013, doi:10.1038/s41589-022-01077-5 (2022).

23 Karvelis, T. & Siksnys, V. Mis-annotation of TnpB: case of TaRGET-ABE. *Nature chemical biology* **19**, 261-262, doi:10.1038/s41589-022-01242-w (2023).

24 Yoon, P. H., Adler, B. A. & Doudna, J. A. To TnpB or not TnpB? Cas12 is the answer. *Nature chemical biology* **19**, 263-264, doi:10.1038/s41589-022-01243-9 (2023).

25 Nakagawa, R. *et al.* Cryo-EM structure of the transposon-associated TnpB enzyme. *Nature* **616**, 390-397, doi:10.1038/s41586-023-05933-9 (2023).

26 Sasnauskas, G. *et al.* TnpB structure reveals minimal functional core of Cas12 nuclease family. *Nature* **616**, 384-389, doi:10.1038/s41586-023-05826-x (2023).

27 Raguram, A., Banskota, S. & Liu, D. R. Therapeutic in vivo delivery of gene editing agents. *Cell* **185**, 2806-2827, doi:10.1016/j.cell.2022.03.045 (2022).

28 Clement, K. *et al.* CRISPResso2 provides accurate and rapid genome editing sequence analysis. *Nature biotechnology* **37**, 224-226, doi:10.1038/s41587-019-0032-3 (2019).

Acknowledgements

We thank technical support from laboratory animal center (Y.D., J.S., T.Z.), optical imaging (L.T., K.S., W.L.) and gene-editing core (R.Y., X.H., X.Z.) facility in Shanghai Center for Brain Science and Brian-Inspired Technology as well as Lingang Laboratory. **Funding:** This work was funded by Lingang Laboratory (LG2023 to C.X.), and Shanghai City Committee of Science and Technology Project (22QA1412300 to C.X., 20ZR1466600 to X.H.). S.M. was funded by National Natural Science Foundation of China (32100641). H.Y. was funded by National Science and Technology Innovation 2030 Major Program (2021ZD0200900) (H.Y.), Chinese National Science and Technology major project R&D Program of China (2018YFC2000101) (H.Y.), Strategic Priority Research Program of Chinese Academy of Science (XDB32060000) (H.Y.), National Natural Science Foundation of China (31871502, 31901047, 31925016, 91957122 and 82021001) (H.Y.), Basic Frontier Scientific Research Program of Chinese Academy of Sciences From 0 to 1 original innovation project (ZDBS-LY-SM001) (H.Y.), Shanghai Municipal Science and Technology Major Project (2018SHZDZX05) (H.Y.), Shanghai City Committee of Science and Technology Project (18411953700, 18JC1410100, 19XD1424400 and 19YF1455100) (H.Y.) and the International Partnership Program of Chinese Academy of Sciences (153D31KYSB20170059) (H.Y.).

Author contributions: Z.L., R.G. and C.X. jointly conceived the project and designed experiments. Y.Z. and C.X. supervised the whole project. Z.L. and G.L. generated mouse model. Z.L. and R.G. designed vectors, performing in vitro experiments and scanning confocal imaging. X.H. and X.S. assisted with construction plasmids and cell culture. R.Y. and X.Z. prepared AAV virus. R.G., Z.L., Z.S. and G.L. performed in vivo virus injection, tissue dissection, histological immunostaining and liver function experiments. Y.L. and Y.Z. performed bioinformatics analysis. R.G., G.L. and X.H. assisted with tissue dissection, immunostaining and animal breeding. Z.L., R.G., G.L., C.H., Y.Z.

and C.X. analyzed the data and organized figures. Z.L., C.H., Y.Z. and C.X. wrote the manuscript with data contributed by all authors participated in project. **Competing interests:** H.Y. is a founder of HuidaGene Therapeutics. The remaining authors declare no competing interests. **Data and materials availability:** Deep-seq data is deposited to the GEO repository under accession number PRJNA963402 and plasmids are available from the corresponding authors upon request.

Supplementary Materials:

Materials and Methods

Figures S1 to S6

Tables S1 to S3

Fig.1

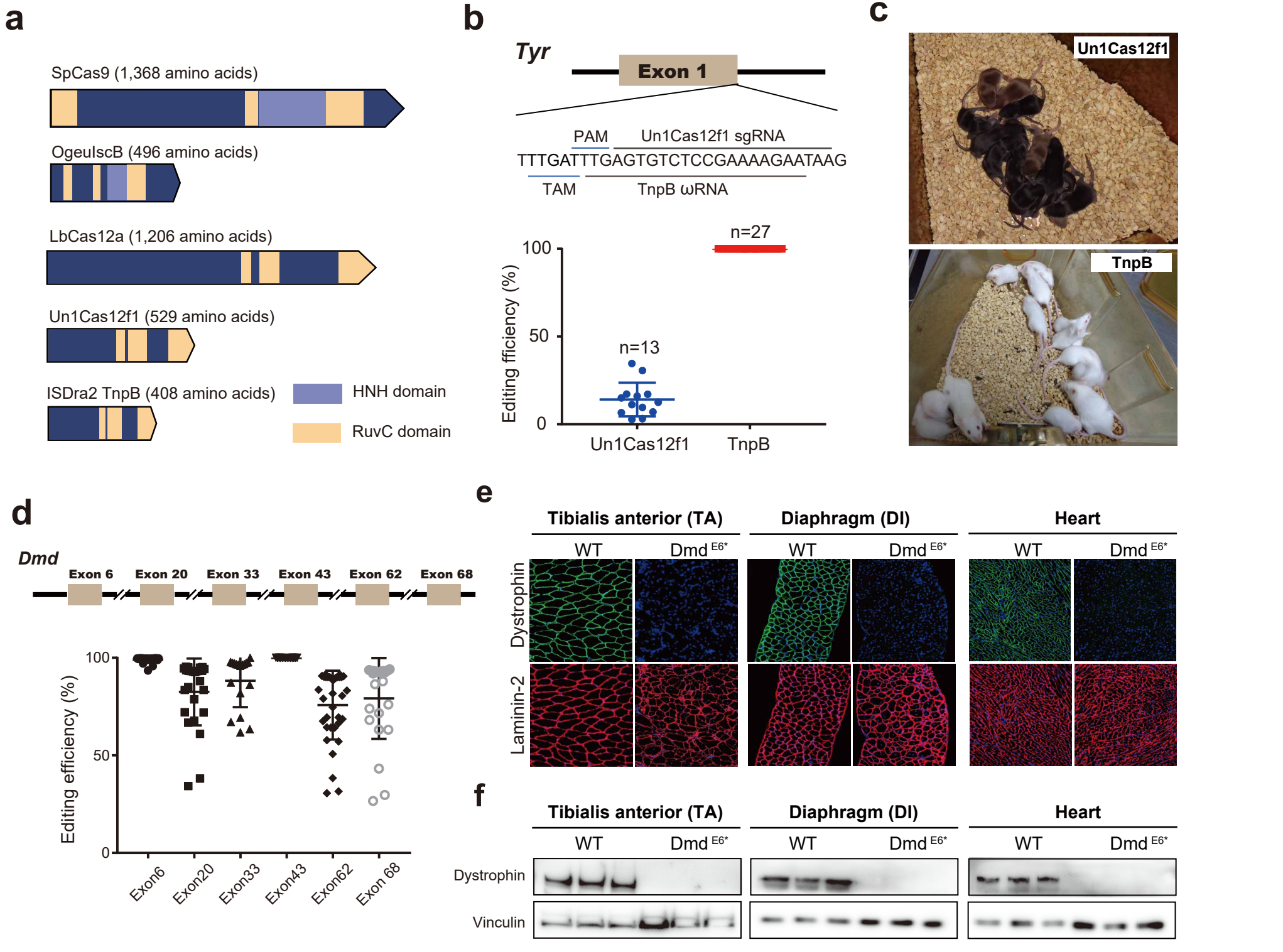
a
SpCas9 (1,368 amino acids)
OgeuIscB (496 amino acids)
LbCas12a (1,206 amino acids)
Un1Cas12f1 (529 amino acids)
ISDra2 TnpB (408 amino acids)
HNH domain
RuvC domain
b
Tyr
Exon 1
PAM
Un1Cas12f1 sgRNA
TTTGATTTGAGTGTCTCCGAAAAGAATAAG
TAM
TnpB ωRNA
Editing fficiency (%)
100
50
0
n=27
n=13
Un1Cas12f1
TnpB
c
Un1Cas12f1
TnpB
d
Dmd
Exon 6
Exon 20
Exon 33
Exon 43
Exon 62
Exon 68
Editing efficiency (%)
100
50
0
Exon6
Exon20
Exon33
Exon43
Exon62
Exon 68
e
Tibialis anterior (TA)
Diaphragm (DI)
Heart
WT
Dmd E6*
Dystrophin
Laminin-2
f
Tibialis anterior (TA)
Diaphragm (DI)
Heart
WT
Dmd E6*
Dystrophin
Vinculin

Main figures and legend

Fig. 1. Mouse embryo injection of TnpB-ωRNA induced efficient gene editing.

a. Characteristics of SpCas9, IscB, LbCas12a, Un1Cas12f1 and TnpB nucleases. **b.** Comparison of editing efficiency between TnpB and Cas12f1 on Tyr gene for gene modified mice. **c.** Coat color phenotype of *Tyr* gene modified mice by Un1Cas12f1 and TnpB. **d.** TnpB-mediated gene editing efficiency for *Dmd* gene. **e.** Dystrophin and laminin-2 immunostaining for TA, DI and heart muscle tissues in wildtype and *Dmd*-edited mice by TnpB. **f.** Western blotting of dystrophin and vinculin protein for three muscle tissues in wild-type and *Dmd*-edited mice by TnpB. Data are represented as means ± SEM. A dot represents a biological replicate. Significant differences between conditions are indicated by asterisk. Unpaired two-tailed Student's t tests. * $P < 0.05$, *** $P < 0.001$, NS non-significant. Scale bars, 200 μm.

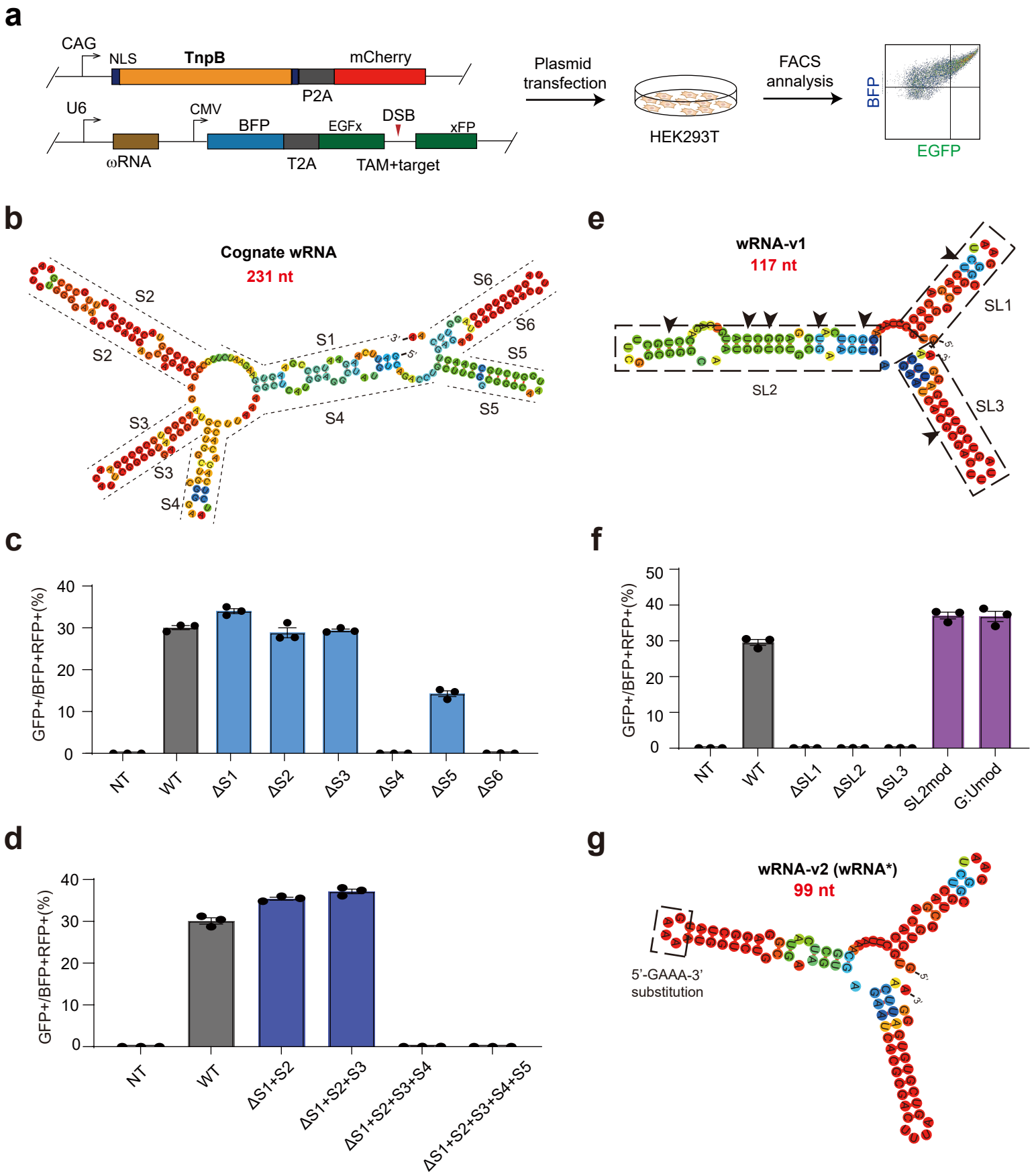

Fig. 2. Stepwise engineering of TnpB-associated ωRNA improved gene editing efficiency.

a. Reporter assay schematics of detecting cleavage activity of TnpB-ωRNA. **b.** Predicted secondary structure of cognate ωRNA (245 nt). Cognate ωRNA was divided into 6 segments, named from S1 to S6. **c.** Reporter assay results using engineered ωRNA by one-by-one truncation of S1 to S6. **d.** Reporter assay results with engineered ωRNA by different combined truncations of S1 to S5. **e.** Predicted secondary structure of a ωRNA variant with simultaneous truncation of S1, S2 and S3. **f.** Reporter assay results for ωRNA variants with different SL deletion and modifications. **g.** Predicted secondary structure of final optimized ωRNA variant. Data are represented as means ± SEM. A dot represents a biological replicate. Significant differences between conditions are indicated by asterisk. Unpaired two-tailed Student's t tests. * $P < 0.05$, *** $P < 0.001$, NS non-significant.

Fig.3

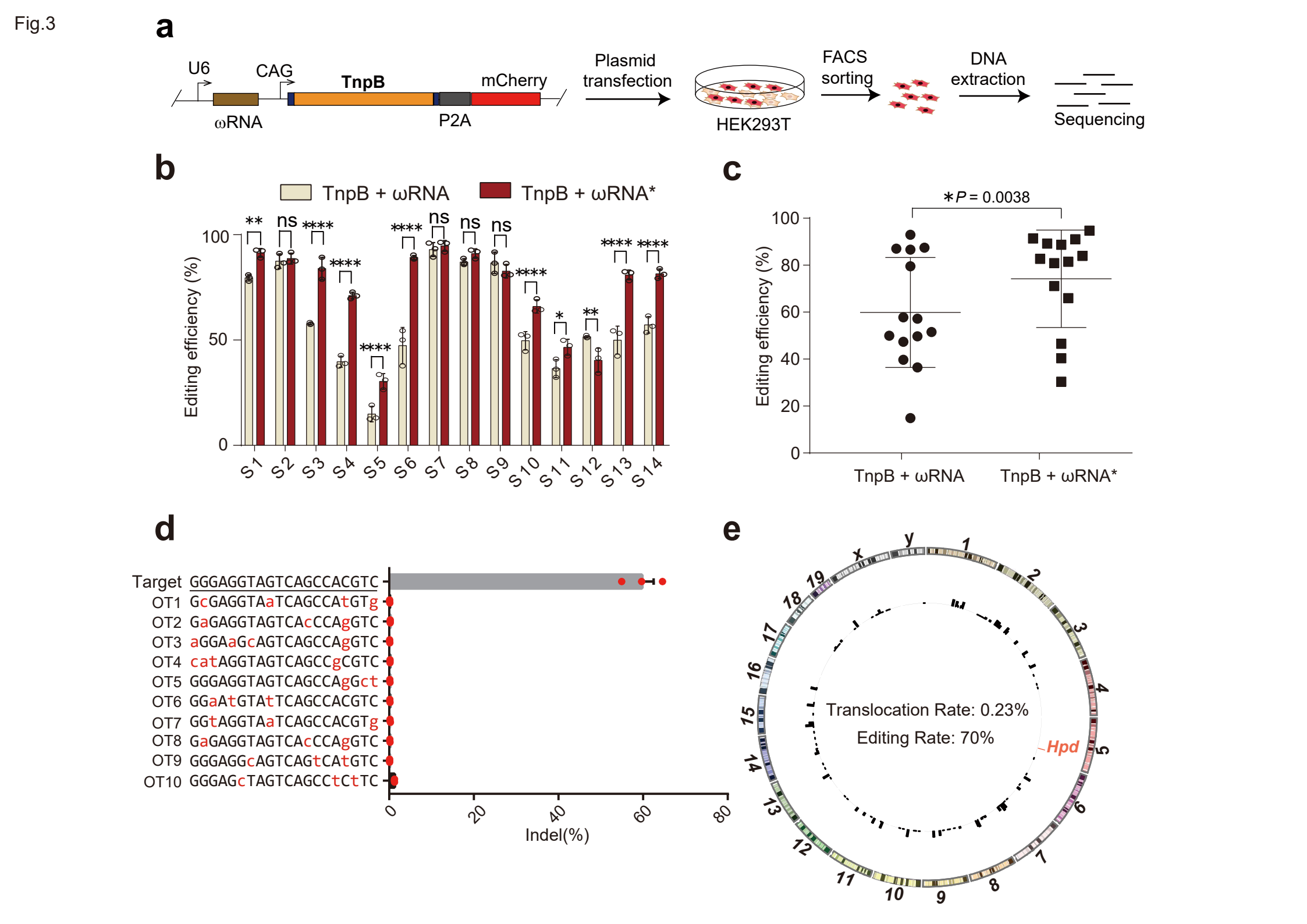
a
U6
CAG
TnpB
mCherry
ωRNA
P2A
Plasmid transfection
HEK293T
FACS sorting
DNA extraction
Sequencing
b
TnpB + ωRNA
TnpB + ωRNA*
Editing efficiency (%)
S1 S2 S3 S4 S5 S6 S7 S8 S9 S10 S11 S12 S13 S14
c
*P = 0.0038
Editing efficiency (%)
TnpB + ωRNA
TnpB + ωRNA*
d
Target GGGAGGTAGTCAGCCACGTC
OT1 GcGAGGTAaTCAGCCAtGTg
OT2 GaGAGGTAGTCAcCCAgGTC
OT3 aGGAaGcAGTCAGCCAgGTC
OT4 catAGGTAGTCAGCCgCGTC
OT5 GGGAGGTAGTCAGCCAgGct
OT6 GGaAtGTAtTCAGCCACGTC
OT7 GGtAGGTAaTCAGCCACGTg
OT8 GaGAGGTAGTCAcCCAgGTC
OT9 GGGAGGcAGTCAGtCAtGTC
OT10 GGGAGcTAGTCAGCCtCtTC
Indel(%)
e
Translocation Rate: 0.23%
Editing Rate: 70%
Hpd

Fig. 3. Characterization of endogenous gene editing activity and off-target effect with optimized TnpB-ωRNA system.

a. The experimental workflow for detecting editing efficiency of original and optimized TnpB-ωRNA in HEK293T cells. **b.** Efficiency comparison results for 14 endogenous gene edited with original and optimized TnpB-ωRNA. **c.** Summary results for 14 endogenous genes editing efficiency. **d.** Off-target analysis for top predicted off-target genomic loci via Cas-OFFinder. **e.** Genome-wide off-target analysis with PEM-seq. Data are represented as means ± SEM. A dot represents a biological replicate. Significant differences between conditions are indicated by asterisk. Unpaired two-tailed Student's t tests. * $P < 0.05$, *** $P < 0.001$, NS non-significant.

Fig.4

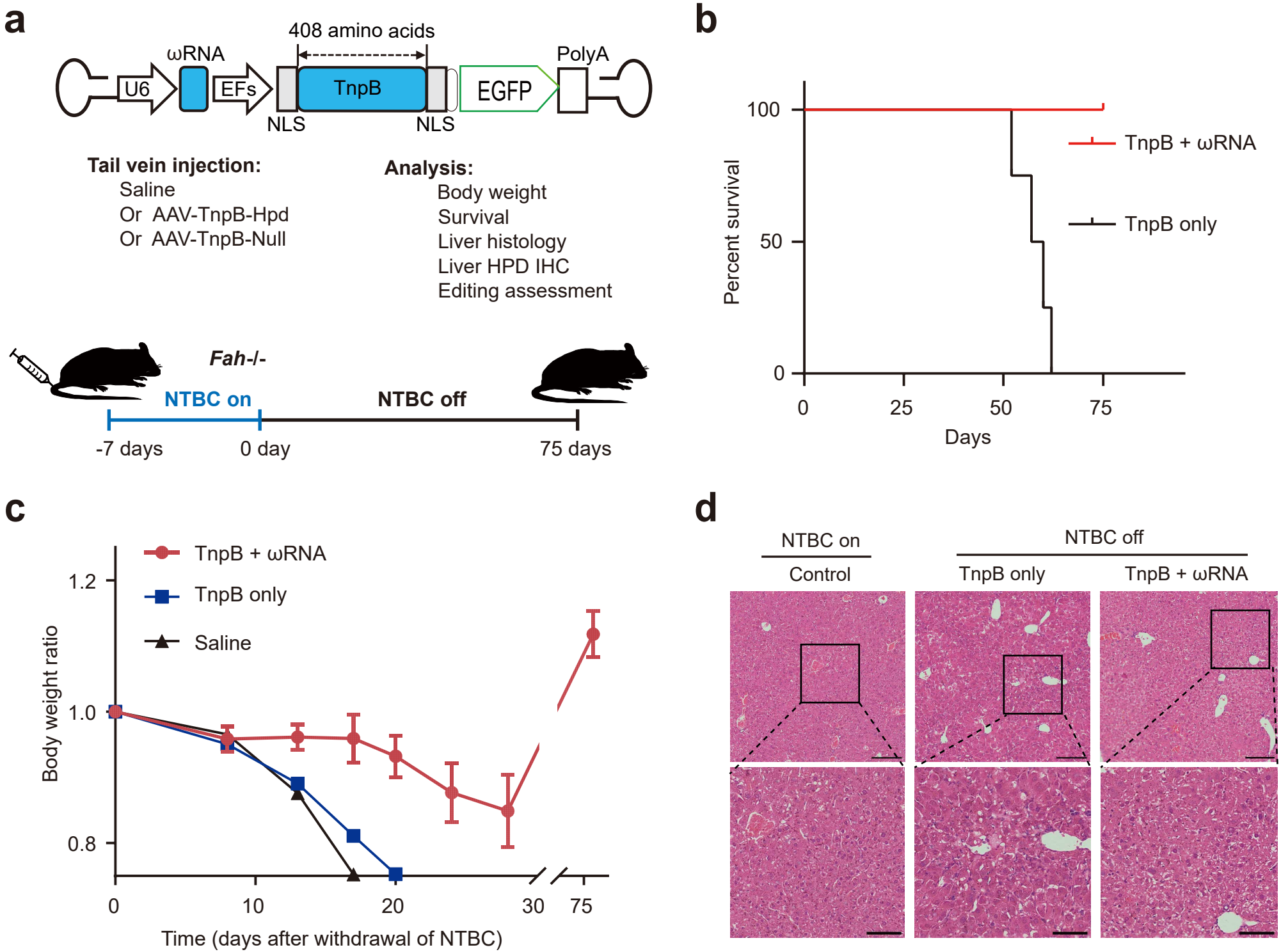
a
408 amino acids
ωRNA
U6
EFs
TnpB
NLS
NLS
EGFP
PolyA
Tail vein injection:
Saline
Or AAV-TnpB-Hpd
Or AAV-TnpB-Null
Analysis:
Body weight
Survival
Liver histology
Liver HPD IHC
Editing assessment
Fah-/-
NTBC on
NTBC off
-7 days
0 day
75 days
b
Percent survival
100
50
0
0
25
50
75
Days
TnpB + ωRNA
TnpB only
c
TnpB + ωRNA
TnpB only
Saline
Body weight ratio
1.2
1.0
0.8
0
10
20
30
75
Time (days after withdrawal of NTBC)
d
NTBC on
NTBC off
Control
TnpB only
TnpB + ωRNA

Fig. 4. Prevention of fatal liver disease with in vivo delivery of TnpB-ωRNA via single AAV.

a. Diagram of AAV-TnpB-ωRNA vector and gene therapy schematics in Fah-/- mouse model of type I hereditary tyrosinaemia. **b.** Survival curve for disease mice treated with AAV-TnpB-ωRNA or AAV-TnpB without ωRNA. **c.** Body weight change during the observation period for disease mice in different treatment groups. **d.** Histology analysis with H&E staining for mouse liver from different treatment groups. Data are represented as means ± SEM. A dot represents a biological replicate. Significant differences between conditions are indicated by asterisk. Unpaired two-tailed Student's t tests. * $P < 0.05$, *** $P < 0.001$, NS non-significant. Scale bars, 200 μm.

Supplementary materials for

Title: Engineering transposon-associated TnpB-ωRNA system for efficient gene editing and disease treatment in mouse

Authors:

Zhifang Li[1†], Ruochen Guo[1,6†], Xiaozhi Sun[1,2†],Guoling Li[5†], Yuanhua Liu[6], Xiaona Huo[1,2], Rongrong Yang[1,2], Zhuang Shao[1], Hainan Zhang[4], Weihong Zhang[4], Xiaoyin Zhang[1,2], Shuangyu Ma[7], Yinan Yao[6], Xinyu Liu[6], Hui Yang[3,4,6], Chunyi Hu[5*], Yingsi Zhou[4*], Chunlong Xu[1,2,3*]

†These authors contributed equally to this work.

***Correspondences:** hu_dbs@nus.edu.sg (C.H.), yingsizhou@huidagene.com (Y.Z.), xucl@lglab.ac.cn (C.X.)

This PDF file includes:

Materials and Methods

Study approval

The objectives of the present study were to show proof-of-concept for in vivo TnpB-mediated gene editing in wildtype and disease mice. All animal experiments were performed and approved by the Animal Care and Use Committee of Shanghai Center for Brain Science and Brian-Inspired Technology, Shanghai, China.

Plasmid constructions

The pCBh-TnpB-hU6-BpiI plasmid encoded a human codon-optimized TnpB driven by CBh promoter, and hU6-driven ωRNAs with *Bpi*I cloning site. The sgRNA and ωRNA were designed suitable for Un1Cas12f1 and TnpB, then synthesized as DNA oligonucleotides and cloned into pCBh-Un1Cas12f1 or pCBh-TnpB to get the CRISPR targeting plasmids.

Cell culture, transfection and flow cytometry analysis

HEK293T were maintained in Dulbecco's modified eagle medium (DMEM) (Gibco, 11965092) supplemented with 10% fetal bovine serum at 37 °C and 5% CO_2 in a humidified incubator. For sgRNA screening, CRISPR targeting plasmids and reporter were co-transfected using polyethylenimine (PEI) transfection reagent. After transfected cells were cultured with 48 hours, we carefully resuspended the cell pellet, and then analyzed or sorted by BD FACSAria II. Flow cytometry results were analyzed with FlowJo X (v.10.0.7).

In vitro transcription of TnpB and ωRNA

TnpB mRNA was transcribed using the mMESSAGE mMACHINE T7 Ultra Kit (Invitrogen, AM1345). T7 promoter was added to ωRNA template by PCR amplification of pCX2280 using primer F and R. The PCR products purified with Omega gel extraction Kit (Omega, D2500-02), templates were transcribed using the MEGAshortscript Kit (Invitrogen, AM1354). The TnpB

mRNA and ωRNA were purified by MEGAclear Kit (Invitrogen, AM1908), eluted with RNase-free water and stored at -80°C.

Zygote injection and embryo transplantation

Eight-week-old B6D2F1 female mice were super ovulated and mate with B6D2F1 male mice, and fertilized embryos were collected from oviduct. The mixture of TnpB mRNA(50 ng/μL) and ωRNA (100 ng/μL) was injected into the cytoplasm of fertilized eggs using a FemtoJet microinjector(Eppendrof). The injected embryos were cultured in KOSM medium with amino acids at 37°C under 5% CO_2 in a humidified incubator overnight and then transferred into oviducts of pseudo-pregnant ICR foster mothers at 0.5-d.p.c.

AAV virus production

The adeno-associated virus 8 (AAV8) serotype was used in this study. The TnpB plasmids with ωRNA was sequenced before packaging into AAV8 vehicle, and the AAV vectors were packaged by transfection of HEK293T cell with helper plasmids. The virus titer was 5×10^{13} (AAV-TnpB), and 5×10^{13} (AAV-TnpB-ωRNA) genome copies/mL as determined by qPCR specific for the inverted terminal repeat.

Gene editing treatment for tyrosinaemia mouse model

Mice were housed in a barrier facility with a 12-hour light/dark cycle and 18–23 °C with 40–60% humidity. Diet and water were accessible at all times. $Fah^{-/-}$ mice were kept on 10mg/L NTBC (Sigma-Aldrich, Cat. No. PHR1731) in drinking water when indicated. For hydrodynamic liver injection, AAV8 (4×10^{11} vg/mouse) in 200 μl saline were injected via the tail vein into 8-10 weeks old male and female mice. Mice were kept off NTBC water at 7 days post injection, and their body weights were recorded every 3-5 days. Mice were harvested at 75 days after NTBC water withdrawal for histology and DNA analysis. Control mice off NTBC water were harvested when reaching >20%

563 weight loss.

564

565 **Histological analysis and Serum biochemistry**

566 Liver tissues were harvested, and sections were fixed in 4% PFA overnight.
567 The following antibodies were used: anti-HPD antibody (SantaCruz, sc-
568 390279; dilution 1:100), anti-P21 antibody (Abcam, ab109199; dilution 1:200).
569 Immunohistochemistry, immunofluorescence and hematoxylin and eosin
570 (H&E) staining were performed by the standard procedures. Blood was
571 collected using retro-orbital puncture before mice was sacrificed. ALT, AST,
572 tyrosine and bilirubin levels in serum were determined using diagnostic ELISA
573 Kits (Abcam, HWRK chem).

574

575 **Targeted deep sequencing**

576 To analyze TnpB targeting efficiency, the DNA of successfully transfected cells
577 or AAV8 treatment tissues were extracted with TIANamp Genomic DNA
578 Kit(TIANGEN,) according to the manufacturer protocol. DNA was amplified
579 with Phanta max super-fidelity DNA polymerase (Vazyme, P505-d1) for
580 Sanger or deep sequencing methods. And deep sequencing libraries were
581 used to add Illumina flow cell binding sequences and specific barcodes on the
582 5′ and 3’ end of the primer sequence. The products were pooled and
583 sequenced with 150 paired-end reads on an Illumina Hiseq instrument.
584 FASTQ format data were analyzed using the Cutadapt (v.2.8)41 according to
585 assigned barcode sequences. CRISPResso2 was used for gene editing
586 analysis[28].

587

588 **PEM-seq analysis**

589 Genome-wide off-target analysis was performed following PEM-seq protocol
590 previously described[16]. The 20 μg genomic DNA from TnpB edited or control
591 samples were fragmented with Covaris sonicator to generate 300-700 bp
592 DNA. DNA fragments was tagged with biotin at 5’-end by one-round PCR

extension using a biotinylated primer, primer leftover removed by AMPure XP beads and purified by streptavidin beads. The single-stranded DNA on streptavidin beads is ligated with a bridge adapter containing 14-bp random molecular barcode, and PCR product was generated via nested PCR to enrich DNA fragment containing the bait DSB events and tagged with illumine adapter sequences. The prepared sequencing library was sequenced by Hi-seq 2500 with 150 bp pair-end reads. PEM-seq data analysis was performed using PEM-Q pipeline with default parameters.

Statistical analysis

The number of independent biological replicates were shown in the figure legend. The data are presented as means ± SEM. Differences were assessed using unpaired two-tailed Student's t tests. Differences in means were considered statistically significant at $P < 0.05$.

Fig.S1

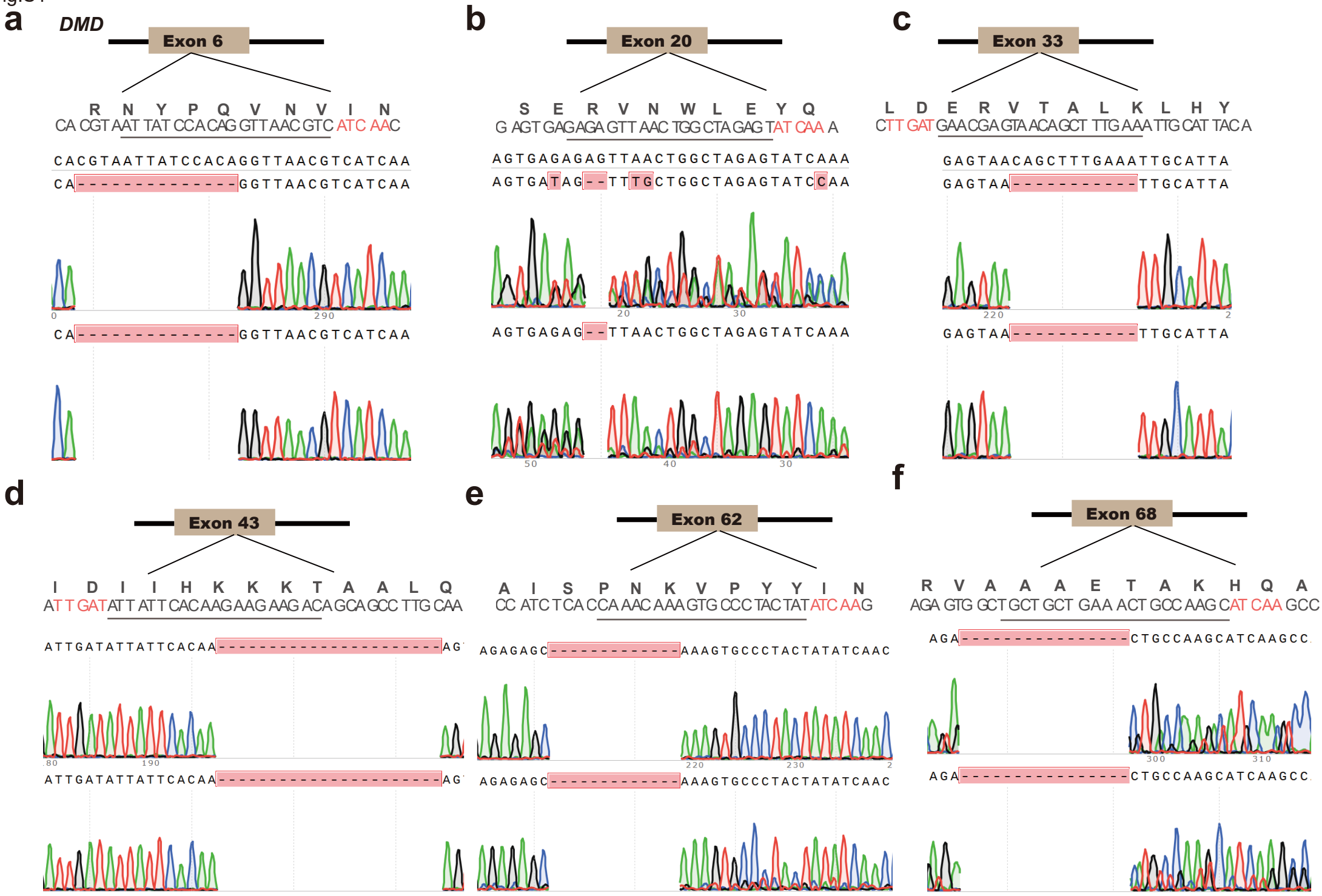
a
DMD
Exon 6
R N Y P Q V N V I N
CA CGT AAT TAT CCA CAG GTT AAC GTC ATC AAC
CACGTAATTATCCACAGGTTAACGTCATCAA
CA----------GGTTAACGTCATCAA
0
290
CA----------GGTTAACGTCATCAA
b
Exon 20
S E R V N W L E Y Q
G AGT GAG AGA GTT AAC TGG CTA GAG TAT CAA A
AGTGAGAGAGTTAACTGGCTAGAGTATCAAA
AGTGATAG--TTTGCTGGCTAGAGTATCCAA
20
30
AGTGAGAG--TTAACTGGCTAGAGTATCAAA
50
40
30
c
Exon 33
L D E R V T A L K L H Y
CTT GAT GAA CGA GTA ACA GCT TTG AAA TTG CAT TAC A
GAGTAACAGCTTTGAAATTGCATTA
GAGTAA----------TTGCATTA
220
2
GAGTAA----------TTGCATTA
d
Exon 43
I D I I H K K K T A A L Q
ATT GAT ATT ATT CAC AAG AAG AAG ACA GCA GCC TTG CAA
ATTGATATTATTCACAA----------AG
80
190
ATTGATATTATTCACAA----------AG
e
Exon 62
A I S P N K V P Y Y I N
CC ATC TCA CCA AAC AAA GTG CCC TAC TAT ATC AAG
AGAGAGC----------AAAGTGCCCTACTATATCAAC
220
230
2
AGAGAGC----------AAAGTGCCCTACTATATCAAC
f
Exon 68
R V A A A E T A K H Q A
AGA GTG GCT GCT GCT GAA ACT GCC AAG CAT CAA GCC
AGA----------CTGCCAAGCATCAAGCC
300
310
AGA----------CTGCCAAGCATCAAGCC

Supplementary figures and legend

Fig. S1. Transcriptional genotyping of *Dmd*-edited mice with RT-PCR.

a-f. RT-PCR and sequencing results for muscle from individual mouse edited by TnpB in exon 6, 20, 33, 43, 62 and 68 of *Dmd* gene.

Fig.S2

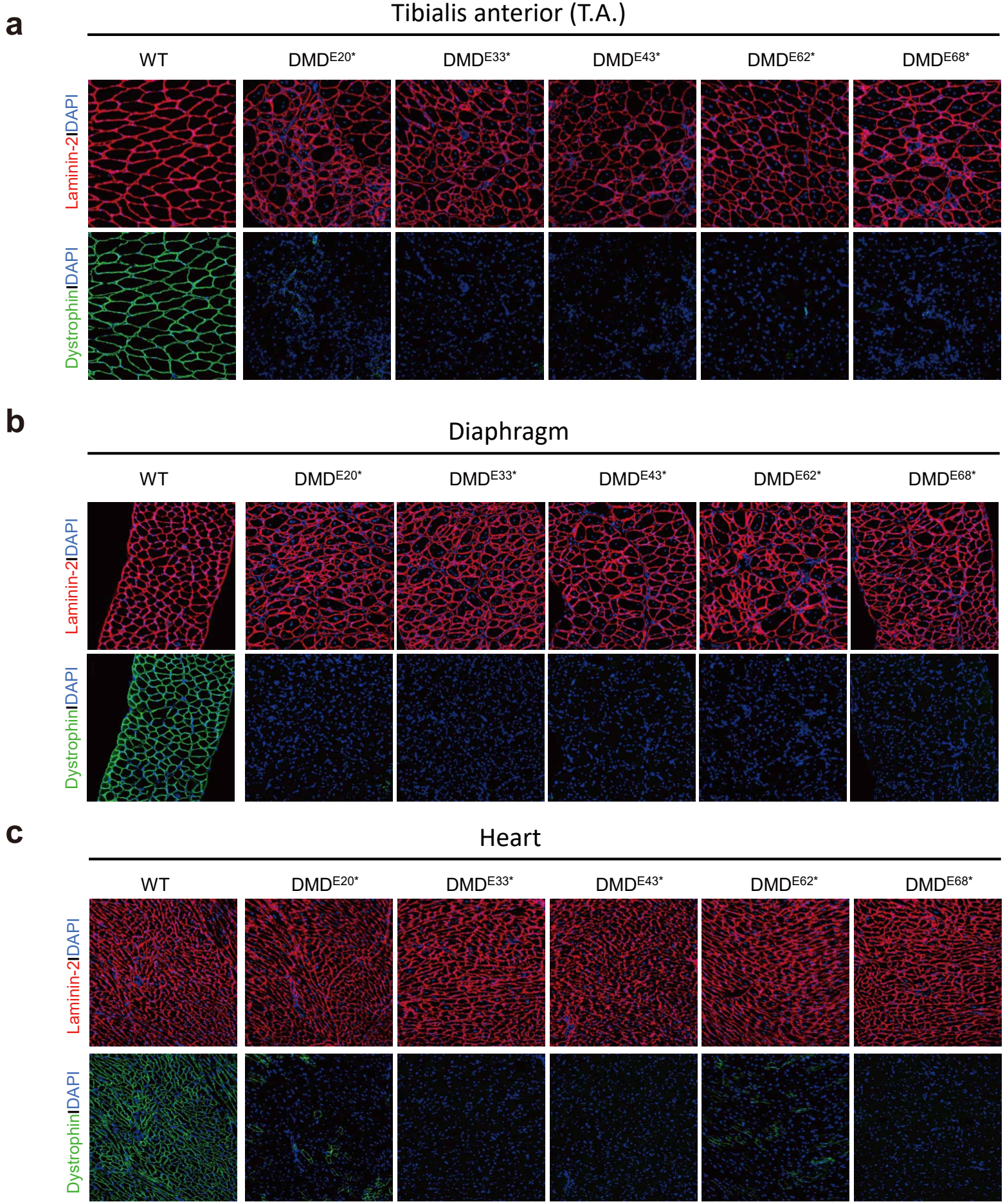

627 **Fig. S2. Dystrophin and laminin-2 immunostaining results for TA, DI and**
628 **heart muscle in *Dmd*-edited mice.**

629 **a-c.** Immunostaining of dystrophin and laminin-2 in TA, DI and heart muscle
630 from mice edited by TnpB in exon 6, 20, 33, 43, 62 and 68 of *Dmd* gene. Scale
631 bars, 200 μm.

632

Fig.S3

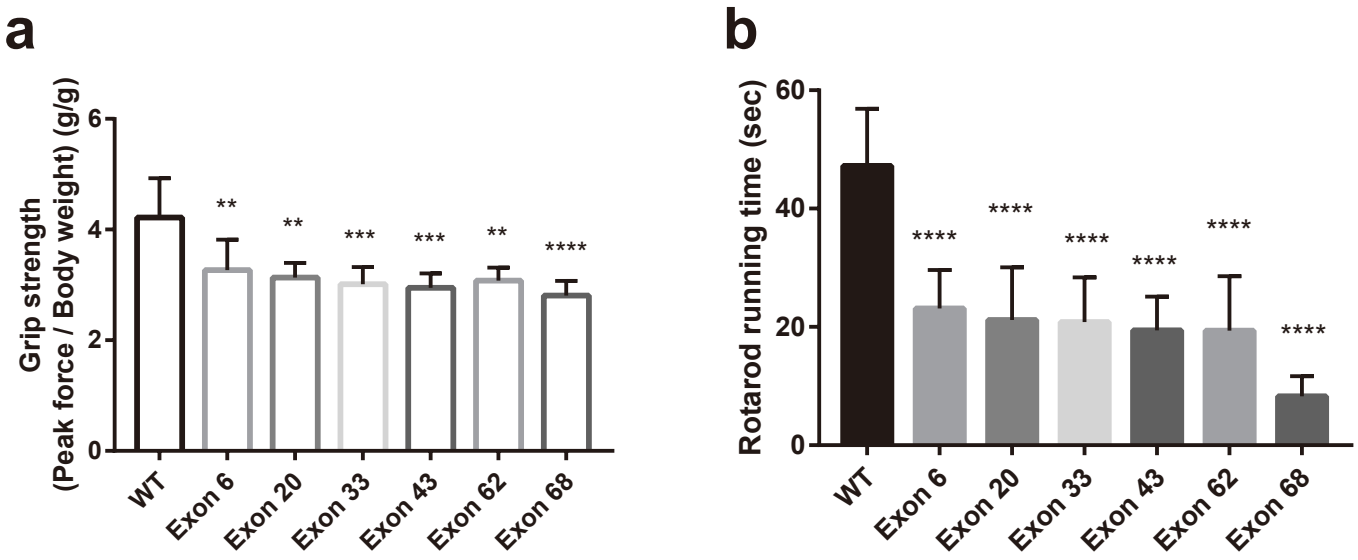

Fig. S3. Grip strength and rotarod test for *Dmd*-edited mice.

a. Forelimb grip strength analysis results for wildtype and *Dmd* mutant mice. **b.** Rotarod running time analysis results for wildtype and *Dmd* mutant mice. Data are represented as means ± SEM. A dot represents a biological replicate. Significant differences between conditions are indicated by asterisk. Unpaired two-tailed Student's t tests. * $P < 0.05$, *** $P < 0.001$, NS non-significant.

Fig.S4

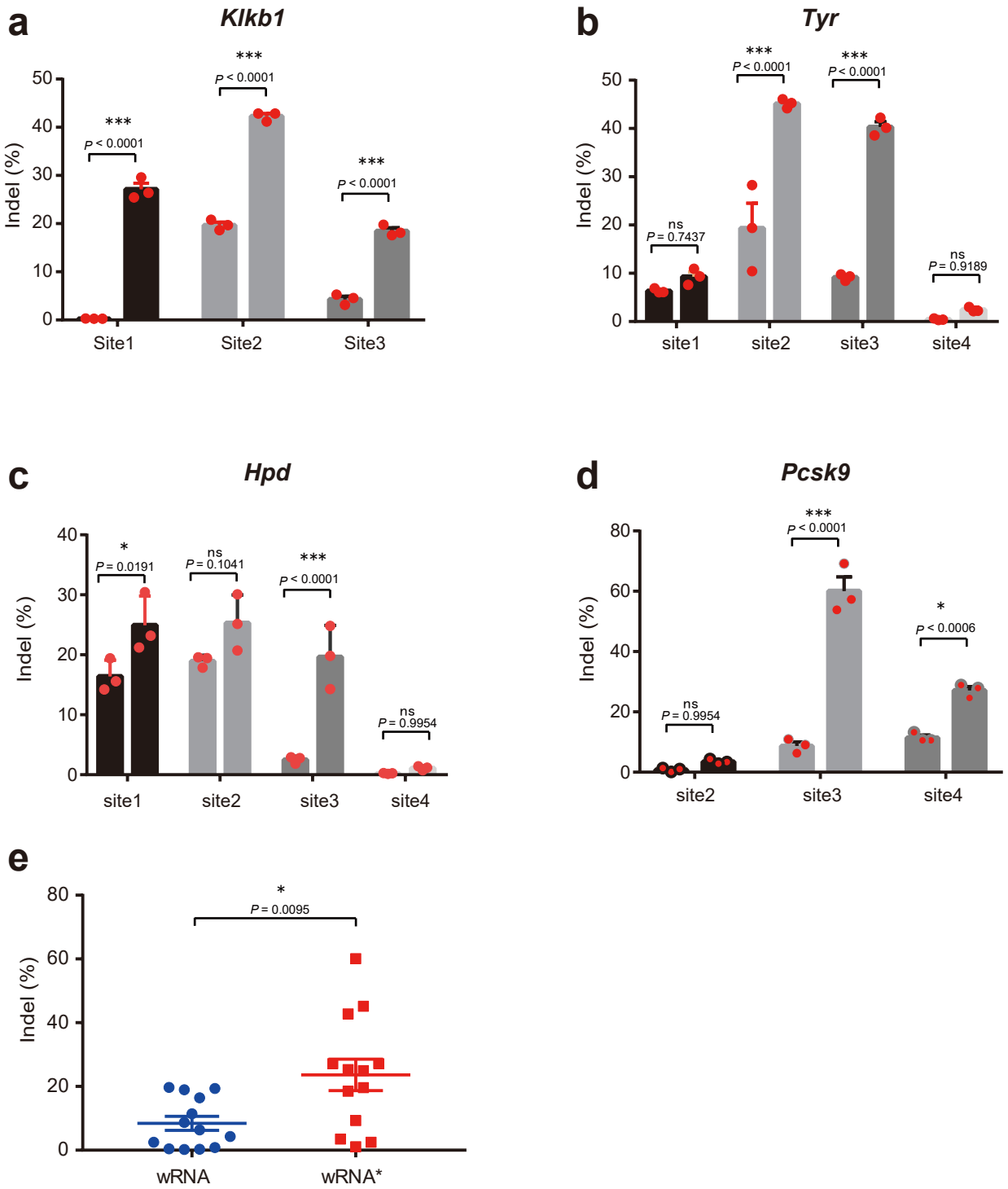
a
Klkb1
Indel (%)
***
P < 0.0001
Site1
Site2
Site3
b
Tyr
ns
P = 0.7437
P = 0.9189
site1
site2
site3
site4
c
Hpd
*
P = 0.0191
ns
P = 0.1041
P = 0.9954
d
Pcsk9
P < 0.0006
e
*
P = 0.0095
wRNA
wRNA*

Fig. S4. Characterization of gene editing activity for engineered TnpB-ωRNA system in mouse N2a cells.

a-d. Efficiency comparison using cognate and engineered ωRNA for mouse *Klkb1, Tyr, Hpd,* and *Pcsk9* gene editing. **b.** Summary statistic results for gene editing activity characterization of cognate and engineered ωRNA in N2a. Data are represented as means ± SEM. A dot represents a biological replicate. Significant differences between conditions are indicated by asterisk. Unpaired two-tailed Student's t tests. * $P < 0.05$, *** $P < 0.001$, NS non-significant.

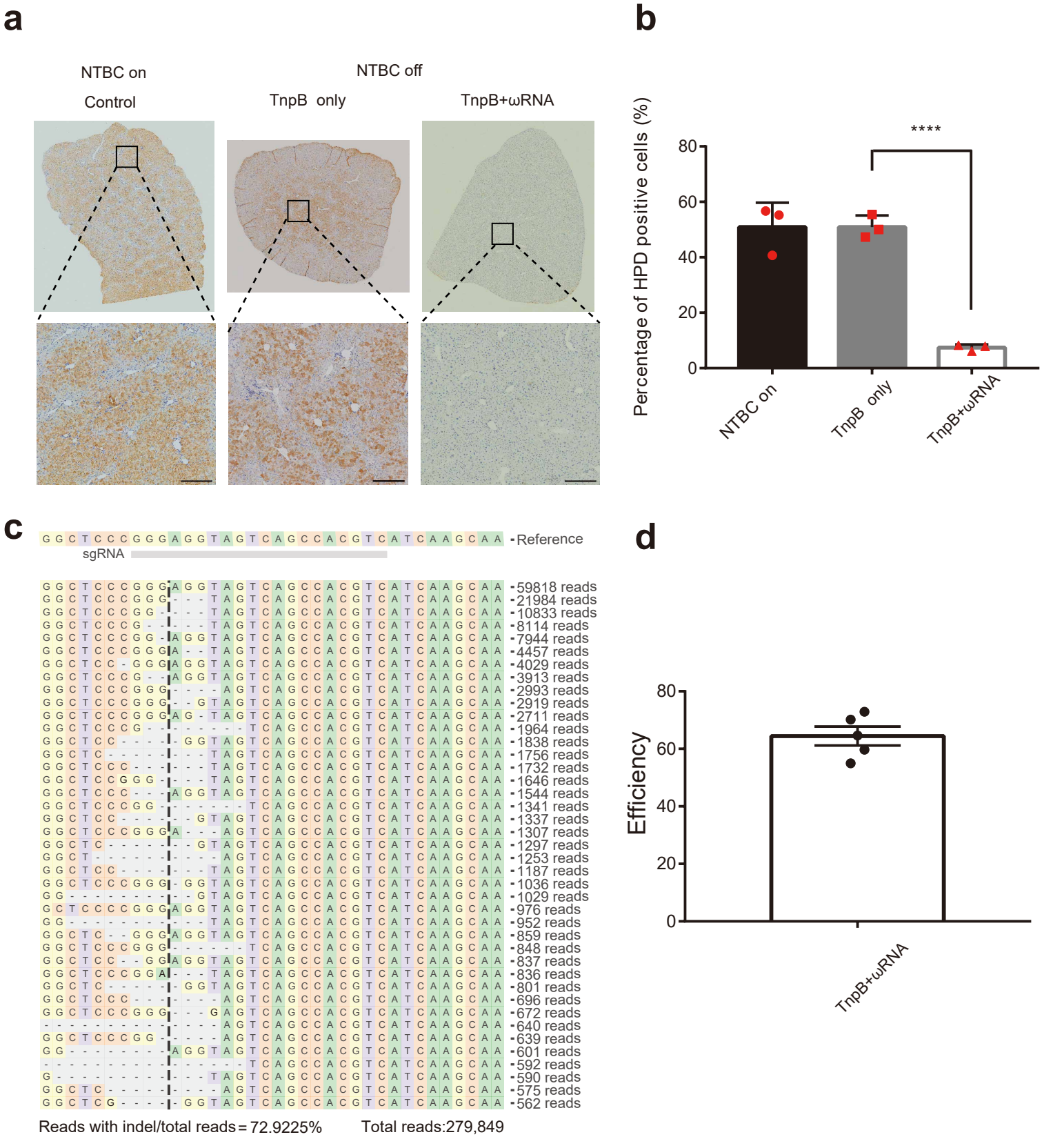

672 **Fig. S5. Gene editing and immunostaining analysis for HPD in AAV-**

673 **TnpB-ωRNA treated mouse liver.**

674 **a.** Hpd immunostaining analysis in $Fah^{-/-}$ mice treated with or without AAV-

675 TnpB-ωRNA. **b.** Deep-seq results for *Hpd* gene editing by AAV-TnpB.

676

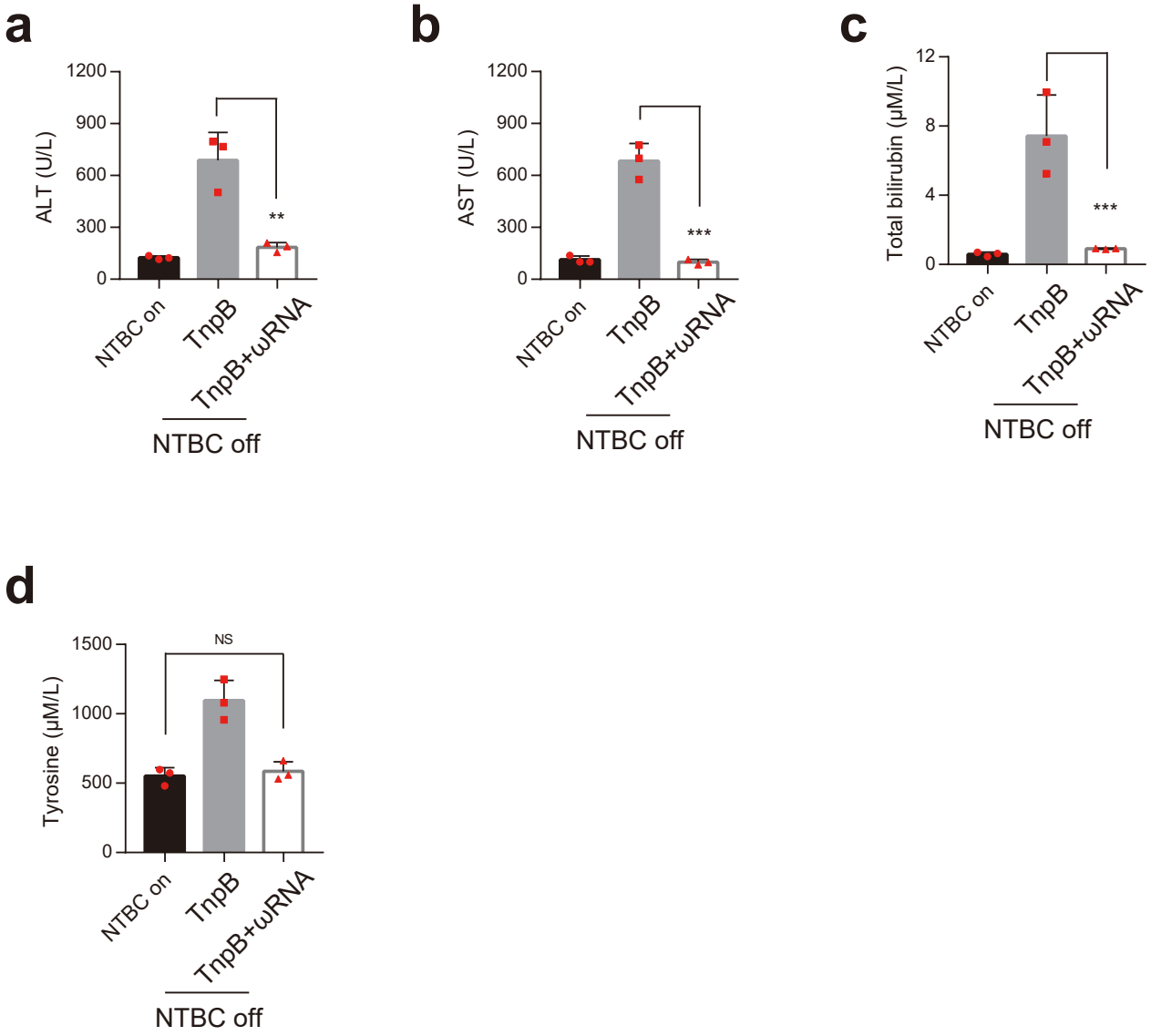

Fig. S6. Serum biochemical analysis for AAV-TnpB-ωRNA treated mouse liver.

a-d. Biochemical analysis of serum indicators for liver metabolic function in TnpB-treated or untreated mice (n=3). Liver damage markers alanine aminotransferase (ALT), aspartate aminotransferase (AST), total bilirubin and tyrosine were measured in peripheral blood from $Fah^{-/-}$ mice injected with AAV-TnpB without or with ωRNA (NTBC off, day 30). $Fah^{-/-}$ mice on NTBC water (NTBC on) served as a control. Data are represented as means ± SEM. A dot represents a biological replicate. Significant differences between conditions are indicated by asterisk. Unpaired two-tailed Student's t tests. * $P < 0.05$, *** $P < 0.001$, NS non-significant.

689 **Supplementary Table S1. Target sgRNA and primer sequence.**

sgRNA	Target site sequences (5'-3')	Primer sequence
HEK1-site1	GTCTTATCACCCTATAGAGT	TCAA GTCTTATCACCCTATAGAGT
		GGCC ACTCTATAGGGTGATAAGAC
HEK1-site2	AATGGAGGTCTGGTGAGTAT	TCAA AATGGAGGTCTGGTGAGTAT
		GGCC ATACTCACCAGACCTCCATT
HEK1-site3	TGTTTTATTTATTACACACA	TCAA TGTTTTATTTATTACACACA
		GGCC TGTGTGTAATAAATAAAACA
HEK1-site4	TTTACACATCATCATATACA	TCAA TTTACACATCATCATATACA
		GGCC TGTATATGATGATGTGTAAA
HEK1-site5	CTTTTCAAAATTACTTTGCA	TCAA CTTTTCAAAATTACTTTGCA
		GGCC TGCAAAGTAATTTTGAAAAG
HEK1-site6	AGAAGTGAGATGGCTCCAAA	TCAA AGAAGTGAGATGGCTCCAAA
		GGCC TTTGGAGCCATCTCACTTCT
HEK1-site7	GACCCAAAGAAATGTATTCC	TCAA GACCCAAAGAAATGTATTCC
		GGCC GGAATACATTTCTTTGGGTC
HEK1-site8	ATTCAAAAACACGCAAACCC	TCAA ATTCAAAAACACGCAAACCC
		GGCC GGGTTTGCGTGTTTTTGAAT
HEK1-site9	GTGATTTCTTGGAAATAGTT	TCAA GTGATTTCTTGGAAATAGTT
		GGCC AACTATTTCCAAGAAATCAC
HEK1-site10	AAAGAAGTCTACTTTGACTT	TCAA AAAGAAGTCTACTTTGACTT
		GGCC AAGTCAAAGTAGACTTCTTT
HEK1-site11	TCCTTTGCCAGGTTTCTGCA	TCAA TCCTTTGCCAGGTTTCTGCA
		GGCC TGCAGAAACCTGGCAAAGGA
HEK1-site12	TCTGCACAGAGCTCCAAATG	TCAA TCTGCACAGAGCTCCAAATG
		GGCC CATTTGGAGCTCTGTGCAGA
HEK1-site13	AACTAGACCTGTTGCTCAAA	TCAA AACTAGACCTGTTGCTCAAA
		GGCC TTTGAGCAACAGGTCTAGTT
HEK1-site14	TAATTAGAGCATAAATAAGA	TCAA TAATTAGAGCATAAATAAGA
		GGCC TCTTATTTATGCTCTAATTA
HEK1-site15	TTGGGGCTAGCTGTATTCTC	TCAA TTGGGGCTAGCTGTATTCTC
		GGCC GAGAATACAGCTAGCCCCAA
HEK1-site16	GGGTTATGAATATTGACACA	TCAA GGGTTATGAATATTGACACA
		GGCC TGTGTCAATATTCATAACCC
HEK1-site17	TCAAGTACCACCAGTTTTAT	TCAA TCAAGTACCACCAGTTTTAT
		GGCC ATAAAACTGGTGGTACTTGA
HEK1-site18	AACTTTAGATGTCTGTTTCC	TCAA AACTTTAGATGTCTGTTTCC
		GGCC GGAAACAGACATCTAAAGTT
HEK1-site19	AGAACACCCATAAGAACAAC	TCAA AGAACACCCATAAGAACAAC
		GGCC GTTGTTCTTATGGGTGTTCT
HEK1-site20	GAAAAGATTACAGAATCAGG	TCAA GAAAAGATTACAGAATCAGG
		GGCC CCTGATTCTGTAATCTTTTC

HEK1-site21	TATGTCTAGGTGAACTGGTA	TCAA TATGTCTAGGTGAACTGGTA
		GGCC TACCAGTTCACCTAGACATA
HEK1-site22	AGATGATGTTTCCACACATA	TCAA AGATGATGTTTCCACACATA
		GGCC TATGTGTGGAAACATCATCT
HEK1-site23	TTTTAAGGAATTTGACATAT	TCAA TTTTAAGGAATTTGACATAT
		GGCC ATATGTCAAATTCCTTAAAA
HEK1-site24	CCAAGTTCAAAAGTTGTAAT	TCAA CCAAGTTCAAAAGTTGTAAT
		GGCC ATTACAACTTTTGAACTTGG
HEK1-site25	CTGCCTTCAGAAAGCACCTT	TCAA CTGCCTTCAGAAAGCACCTT
		GGCC AAGGTGCTTTCTGAAGGCAG
HEK1-site26	AAAAATGCATGAAGCTCCTT	TCAA AAAAATGCATGAAGCTCCTT
		GGCC AAGGAGCTTCATGCATTTTT
HEK1-site27	TAAGGAACTAGAATCTAAAA	TCAA TAAGGAACTAGAATCTAAAA
		GGCC TTTTAGATTCTAGTTCCTTA
HEK1-site28	CCTTACTGACTTTCAGCTTT	TCAA CCTTACTGACTTTCAGCTTT
		GGCC AAAGCTGAAAGTCAGTAAGG
HEK1-site29	GAGTCCAGTCAGAAAGCAGA	TCAA GAGTCCAGTCAGAAAGCAGA
		GGCC TCTGCTTTCTGACTGGACTC
HEK1-site30	TTCAAGAATATTTTAGCACA	TCAA TTCAAGAATATTTTAGCACA
		GGCC TGTGCTAAAATATTCTTGAA
HEK1-site31	TCTCTCATAATATTTCATTT	TCAA TCTCTCATAATATTTCATTT
		GGCC AAATGAAATATTATGAGAGA
HEK2-site1	ATAAACATTTTATTAACATG	TCAA ATAAACATTTTATTAACATG
		GGCC CATGTTAATAAAATGTTTAT
HEK2-site2	TGAGATTAATTCACATGTGA	TCAA TGAGATTAATTCACATGTGA
		GGCC TCACATGTGAATTAATCTCA
HEK2-site3	TCATGTGTTCAAACAGTTTC	TCAA TCATGTGTTCAAACAGTTTC
		GGCC GAAACTGTTTGAACACATGA
HEK2-site4	GTTGTAGGGTTTTTTGTTTG	TCAA GTTGTAGGGTTTTTTGTTTG
		GGCC CAAACAAAAAACCCTACAAC
HEK2-site5	TCAAAATGATCCTTTATGTA	TCAA TCAAAATGATCCTTTATGTA
		GGCC TACATAAAGGATCATTTTGA
HEK2-site6	TGCAACAAACCAACCATTTT	TCAA TGCAACAAACCAACCATTTT
		GGCC AAAATGGTTGGTTTGTTGCA
HEK2-site7	CCTCAGGGTGGTCAGGGCCA	TCAA CCTCAGGGTGGTCAGGGCCA
		GGCC TGGCCCTGACCACCCTGAGG
HEK2-site8	AAATATGTAATTAAATGTCT	TCAA AAATATGTAATTAAATGTCT
		GGCC AGACATTTAATTACATATTT
HEK2-site9	GAATCAGTGCTGGAGAATGG	TCAA GAATCAGTGCTGGAGAATGG
		GGCC CCATTCTCCAGCACTGATTC
HEK2-site10	GCTTTTTTTCTGCTTCTCCA	TCAA GCTTTTTTTCTGCTTCTCCA
		GGCC TGGAGAAGCAGAAAAAAAGC
HEK2-site11	CTCTGATTTTCATGCAGGTG	TCAA CTCTGATTTTCATGCAGGTG

		GGCC CACCTGCATGAAAATCAGAG
HEK2-site12	CCGTAGCCAGGAAGTTAGAT	TCAA CCGTAGCCAGGAAGTTAGAT
		GGCC ATCTAACTTCCTGGCTACGG
HEK2-site13	TAATGGAGACATTGCCATGC	TCAA TAATGGAGACATTGCCATGC
		GGCC GCATGGCAATGTCTCCATTA
HEK2-site14	CACCTGCCCAAATGTGAGGA	TCAA CACCTGCCCAAATGTGAGGA
		GGCC TCCTCACATTTGGGCAGGTG
HEK2-site15	TTCGCCAGCTCTGATGAGGC	TCAA TTCGCCAGCTCTGATGAGGC
		GGCC GCCTCATCAGAGCTGGCGAA
HEK2-site16	ATGGGGATAGGTGGAGACTA	TCAA ATGGGGATAGGTGGAGACTA
		GGCC TAGTCTCCACCTATCCCCAT
HEK3-site1	TTATTAGCATAAGAGTGTCT	TCAA TTATTAGCATAAGAGTGTCT
		GGCC AGACACTCTTATGCTAATAA
HEK3-site2	CTTTAGTAAAGACAGGCAAC	TCAA CTTTAGTAAAGACAGGCAAC
		GGCC GTTGCCTGTCTTTACTAAAG
HEK3-site3	TACACAGCTGACTCACTCTG	TCAA TACACAGCTGACTCACTCTG
		GGCC CAGAGTGAGTCAGCTGTGTA
HEK3-site4	CAATGCACTTTTAAAATTGT	TCAA CAATGCACTTTTAAAATTGT
		GGCC ACAATTTTAAAAGTGCATTG
HEK3-site5	CAAATTCATCATCTCACCTA	TCAA CAAATTCATCATCTCACCTA
		GGCC TAGGTGAGATGATGAATTTG
HEK3-site6	GCATCCCCCATCCACTATAA	TCAA GCATCCCCCATCCACTATAA
		GGCC TTATAGTGGATGGGGGATGC
HEK3-site7	GGCTCAGCTCAGGAGCACCC	TCAA GGCTCAGCTCAGGAGCACCC
		GGCC GGGTGCTCCTGAGCTGAGCC
HEK3-site8	TTTTCCAGAGTTGAGATGAT	TCAA TTTTCCAGAGTTGAGATGAT
		GGCC ATCATCTCAACTCTGGAAAA
HEK3-site9	CTTCCTCAGATGTTTAGGCA	TCAA CTTCCTCAGATGTTTAGGCA
		GGCC TGCCTAAACATCTGAGGAAG
HEK3-site10	GTCTGTACTTAATAACGAAT	TCAA GTCTGTACTTAATAACGAAT
		GGCC ATTCGTTATTAAGTACAGAC
hVEGFA-site1	GAGGGGAGCTGTGGCTCAGA	TCAA GAGGGGAGCTGTGGCTCAGA
		GGCC TCTGAGCCACAGCTCCCCTC
hVEGFA-site2	GTCTGCAGGCCAGATGAGGG	TCAA GTCTGCAGGCCAGATGAGGG
		GGCC CCCTCATCTGGCCTGCAGAC
hVEGFA-site3	ATTCATTGATCCGGGTTTTA	TCAA ATTCATTGATCCGGGTTTTA
		GGCC TAAAACCCGGATCAATGAAT
hVEGFA-site4	CCGGGTTTTATCCCTCTTCT	TCAA CCGGGTTTTATCCCTCTTCT
		GGCC AGAAGAGGGATAAAACCCGG
hVEGFA-site5	CCTTATATTCCTGTGCCCCT	TCAA CCTTATATTCCTGTGCCCCT
		GGCC AGGGGCACAGGAATATAAGG
hVEGFA-site6	TAGTCATCTTCTCCCCTATC	TCAA TAGTCATCTTCTCCCCTATC
		GGCC GATAGGGGAGAAGATGACTA

hVEGFA-site7	GATGCTTTGCCGTAACCCTT	TCAA GATGCTTTGCCGTAACCCTT
		GGCC AAGGGTTACGGCAAAGCATC
hVEGFA-site8	TGGGAAGAAGGTGGGGAGAA	TCAA TGGGAAGAAGGTGGGGAGAA
		GGCC TTCTCCCCACCTTCTTCCCA
hVEGFA-site9	GTCAGCTAATTCTGACTCCT	TCAA GTCAGCTAATTCTGACTCCT
		GGCC AGGAGTCAGAATTAGCTGAC
hVEGFA-site10	GGTGGAAAGCTTAGGGAAGT	TCAA GGTGGAAAGCTTAGGGAAGT
		GGCC ACTTCCCTAAGCTTTCCACC
hVEGFA-site11	CCGCATAATCTGGAAAGGAA	TCAA CCGCATAATCTGGAAAGGAA
		GGCC TTCCTTTCCAGATTATGCGG
Hpd-site1	CAGGCTTATGGAAACTGTGA	TCAA GACGTGGCTGACTACCTCCC
		GGCC GGGAGGTAGTCAGCCACGTC
Hpd-site2	CATAAGCCTGAAAATGTCTC	TCAA CTTCTCCACCAGGGTGTGTG
		GGCC CACACACCCTGGTGGAGAAG
Hpd-site3	TTGAAGGCCCAAGTGAAGCC	TCAA GGATTCCTCGTAGTTGGTCA
		GGCC TGACCAACTACGAGGAATCC
Hpd-site4	GGGCATTTTGATGGATTCCT	TCAA GGGCATTTTGATGGATTCCT
		GGCC AGGAATCCATCAAAATGCCC
Tyr-site1	TGAAGGCCCAAGTGAAGCCC	TCAA TAGAAGAAACATTTTTGATT
		GGCC AATCAAAAATGTTTCTTCTA
Tyr-site2	GAAGGCCCAAGTGAAGCCCT	TCAA TTGAGTGTCTCCGAAAAGAA
		GGCC TTCTTTTCGGAGACACTCAA
Tyr-site3	AAGGCCCAAGTGAAGCCCTC	TCAA ATCATTAAACATGGGTGTTG
		GGCC CAACACCCATGTTTAATGAT
Tyr-site4	GTCCCTTCTCAAAAAACTTA	TCAA TTTGCCCATGAAGCACCAGG
		GGCC CCTGGTGCTTCATGGGCAAA
Pcsk9-site1	TCCCTTCTCAAAAAACTTAC	TCAA TGATCAGGCGAGCAAGTGTG
		GGCC CACACTTGCTCGCCTGATCA
Pcsk9-site2	TCATCTTTTGTCCCTTCTCA	TCAA GACGTCTTTGGTAGAGAAGT
		GGCC ACTTCTCTACCAAAGACGTC
Pcsk9-site3	GTCATCTTTTGTCCCTTCTC	TCAA TTTGCATTCCAGCCCTGGGG
		GGCC CCCCAGGGCTGGAATGCAAA
Klkb1-site1	AGAAGGGACAAAAGATGACA	TCAA GGCCACACTGCTTTAAAGAA
		GGCC TTCTTTAAAGCAGTGTGGCC
Klkb1-site2	CTTCCACCCGGATAAGATGC	TCAA ATGAGAGGGTCCAACTTTAA
		GGCC TTAAAGTTGGACCCTCTCAT
Klkb1-site3	TATCCCGAGTATCTGGAAGA	TCAA TGCTTCATAGGTGAAACGCA
		GGCC TGCGTTTCACCTATGAAGCA
Dmd-site1	ATATACTTTTTCTTCCAAAT	TCAA ATATACTTTTTCTTCCAAAT
		GGCC ATTTGGAAGAAAAAGTATAT
Dmd-site2	TTGGAATATAATCCTCCACT	TCAA TTGGAATATAATCCTCCACT
		GGCC AGTGGAGGATTATATTCCAA
Dmd-site3	GACGTTAACCTGTGGATAAT	TCAA GACGTTAACCTGTGGATAAT

		GGCC ATTATCCACAGGTTAACGTC
Dmd-site4	TGGAATAGTGTGGTTTCACA	TCAA TGGAATAGTGTGGTTTCACA
		GGCC TGTGAAACCACACTATTCCA
Dmd-site5	CCTGAAGGTTGGTAGATTCT	TCAA CCTGAAGGTTGGTAGATTCT
		GGCC AGAATCTACCAACCTTCAGG
Dmd-site6	GGAGACGGAAGTAAATCTGG	TCAA GGAGACGGAAGTAAATCTGG
		GGCC CCAGATTTACTTCCGTCTCC
Dmd-site7	GAGATGTCAGATCCATCATG	TCAA GAGATGTCAGATCCATCATG
		GGCC CATGATGGATCTGACATCTC
Dmd-site8	GAATCCAGCGGTGATCATGC	TCAA GAATCCAGCGGTGATCATGC
		GGCC GCATGATCACCGCTGGATTC
Dmd-site9	TCTTTCATCCTCAGGTACTG	TCAA TCTTTCATCCTCAGGTACTG
		GGCC CAGTACCTGAGGATGAAAGA
Dmd-site10	CTTTAAAGCCACTTGTCTGA	TCAA CTTTAAAGCCACTTGTCTGA
		GGCC TCAGACAAGTGGCTTTAAAG
Dmd-site11	TGAGTGAACTTAGTTTTTCC	TCAA TGAGTGAACTTAGTTTTTCC
		GGCC GGAAAAACTAAGTTCACTCA
Dmd-site12	GCACTCACCTTTTCCTGAGT	TCAA GCACTCACCTTTTCCTGAGT
		GGCC ACTCAGGAAAAGGTGAGTGC
Dmd-site13	ACTCTAGCCAGTTAACTCTC	TCAA ACTCTAGCCAGTTAACTCTC
		GGCC GAGAGTTAACTGGCTAGAGT
Dmd-site14	GGTGTGAGGGCCAAAGAGAA	TCAA GGTGTGAGGGCCAAAGAGAA
		GGCC TTCTCTTTGGCCCTCACACC
Dmd-site15	GTTTTCCTGAAAGAGGAATG	TCAA GTTTTCCTGAAAGAGGAATG
		GGCC CATTCCTCTTTCAGGAAAAC
Dmd-site16	CAGTTCATCCATGACTCCTC	TCAA CAGTTCATCCATGACTCCTC
		GGCC GAGGAGTCATGGATGAACTG
Dmd-site17	GTTGCACAGGTATGTTTTAT	TCAA GTTGCACAGGTATGTTTTAT
		GGCC ATAAAACATACCTGTGCAAC
Dmd-site18	GAACGAGTAACAGCTTTGAA	TCAA GAACGAGTAACAGCTTTGAA
		GGCC TTCAAAGCTGTTACTCGTTC
Dmd-site19	CAGAACATAGAACAAATCAC	TCAA CAGAACATAGAACAAATCAC
		GGCC GTGATTTGTTCTATGTTCTG
Dmd-site20	GGCAAACCGCGGTGACCACT	TCAA GGCAAACCGCGGTGACCACT
		GGCC AGTGGTCACCGCGGTTTGCC
Dmd-site21	TTTGCTCAATAGGAAATTGA	TCAA TTTGCTCAATAGGAAATTGA
		GGCC TCAATTTCCTATTGAGCAAA
Dmd-site22	CGTGAATTGCAGAAGAAGAA	TCAA CGTGAATTGCAGAAGAAGAA
		GGCC TTCTTCTTCTGCAATTCACG
Dmd-site23	CATCTTCTAAATACTCCTGA	TCAA CATCTTCTAAATACTCCTGA
		GGCC TCAGGAGTATTTAGAAGATG
Dmd-site24	ATTATTCACAAGAAGAAGAC	TCAA ATTATTCACAAGAAGAAGAC
		GGCC GTCTTCTTCTTGTGAATAAT

Dmd-site25	TAAATACCTTCATATCATAA	TCAA TAAATACCTTCATATCATAA
		GGCC TTATGATATGAAGGTATTTA
Dmd-site26	CGAGTTATAAAATCACAGAG	TCAA CGAGTTATAAAATCACAGAG
		GGCC CTCTGTGATTTTATAACTCG
Dmd-site27	GTCTTCCAGATCACCCACCA	TCAA GTCTTCCAGATCACCCACCA
		GGCC TGGTGGGTGATCTGGAAGAC
Dmd-site28	GATCATTTCATTGATGTCTT	TCAA GATCATTTCATTGATGTCTT
		GGCC AAGACATCAATGAAATGATC
Dmd-site29	TGCTGGTTTTGTTTTTCAAA	TCAA TGCTGGTTTTGTTTTTCAAA
		GGCC TTTGAAAAACAAAACCAGCA
Dmd-site30	ATTCTCTGTTATCATGTGTA	TCAA ATTCTCTGTTATCATGTGTA
		GGCC TACACATGATAACAGAGAAT
Dmd-site31	GAAAATGGCCAAAAAATCCT	TCAA GAAAATGGCCAAAAAATCCT
		GGCC AGGATTTTTTGGCCATTTTC
Dmd-site32	CACCTCAGCTTGGCGCAACT	TCAA CACCTCAGCTTGGCGCAACT
		GGCC AGTTGCGCCAAGCTGAGGTG
Dmd-site33	ATAGTAGGGCACTTTGTTTG	TCAA ATAGTAGGGCACTTTGTTTG
		GGCC CAAACAAAGTGCCCTACTAT
Dmd-site34	GCTTGGCAGTTTCAGCAGCA	TCAA GCTTGGCAGTTTCAGCAGCA
		GGCC TGCTGCTGAAACTGCCAAGC
Dmd-site35	CAGAGTAACGGGACTGCAAA	TCAA CAGAGTAACGGGACTGCAAA
		GGCC TTTGCAGTCCCGTTACTCTG
Dmd-site36	TTTATTTTCCAGAGATGATG	TCAA TTTATTTTCCAGAGATGATG
		GGCC CATCATCTCTGGAAAATAAA
Dmd-site37	TTCCTTAGAGAGTGAGGAAA	TCAA TTCCTTAGAGAGTGAGGAAA
		GGCC TTTCCTCACTCTCTAAGGAA

690 **Supplementary Table S2. PCR and IVT primers used in this study.**

Primer	Primer sequences (5'-3')
lzf256-mTyr -1f	AACAGGCTGAGAGTATTTGATGT
lzf257-mTyr -1r	CTATATAGTGCATCTTACCTGCC
lzf258-mTyr -2f	GTTGCTGGAAAAGAAGTCTG
lzf259-mTyr -2r	CTCATCTGTGCAAATGTCAC
lzf346-mPcsk9-Exon4-1f	TCAGTTTACCTCCTGGTTCTGTC
lzf347-mPcsk9-Exon4-1r	ACATGTGACAACACTGTAAGAGC
lzf348-mPcsk9-Exon4-2f	CATGAGCCGTCTAATGCGTG
lzf349-mPcsk9-Exon4-2r	TCAGTTTCCCACCTGCATTC
lzf358-mPcsk9-Exon9-1f	GAGCGTTAGTTGGGACCAGAAAG
lzf359-mPcsk9-Exon9-1r	GCCTGCCATACACAAATGCACAC
lzf360-mPcsk9-Exon9-2f	TACAGAGTCTGAGCTGCATG
lzf361-mPcsk9-Exon9-2r	GCTACCCTGACACATGGACC
lzf1121_mHpd-exon3-1f	CAATCAGGGTCCCCAAGGACCTT
lzf1122_mHpd-exon3-1r	GAGAAGTTTGAAACCAGGAAGAT

lzf1123_mHpd-exon3-2f	AGAGTCTCCAAATGACGGAC
lzf1124_mHpd-exon3-2r	TACATCTTGGAACCAGCTAG
lzf1127_mHpd-exon7-1f	CTGAGTTAGGGTCAGCTTCATGG
lzf1128_mHpd-exon7-1r	AAATGACGGAGCTGCCTGTGAAC
lzf1129_mHpd-exon7-2f	TAGAGAAGAGTGGGGGCTTT
lzf1130_mHpd-exon7-2r	GTTTCCCACCAGATGCTTAC
lzf1135_mHpd-exon9-1f	TGAGGATCCTGTGTAACGGGTGT
lzf1136_mHpd-exon9-1r	GTTTGTGGGAGAGGAAAGGGACG
lzf1137_mHpd-exon9-2f	GAAGAGGGTGGGAAGGTCTC
lzf1138_mHpd-exon9-2r	CGCTACTCTCATCGGCAGAG
lzf2045_mDmd-sgRNA1-1f	CTTGAAGGCAATAGCCTTTATAG
lzf2046_mDmd-sgRNA1-1r	GATAATAAAGTAGATAAATGACG
lzf2047_mDmd-sgRNA1-2f	GAAGTTTATTGGCTTCTCAT
lzf2048_mDmd-sgRNA1-2r	TGTAATCAATCTGCCTACTC
lzf2051_mDmd-sgRNA2-1f	CAATTAGTTATTTTCTATCTATT
lzf2052_mDmd-sgRNA2-1r	TAGTCCTAGAAAGATGGTTAGAT
lzf2053_mDmd-sgRNA2-2f	TAGTGAATATAGGAAGCACT
lzf2054_mDmd-sgRNA2-2r	GATATATTAATGATATTGGT
lzf2057_mDmd-sgRNA3-1f	TCTTATTAAAGCATGACAGATGC
lzf2058_mDmd-sgRNA3-1r	TAACAGCATGCAGCCTAGTAGAG
lzf2059_mDmd-sgRNA3-2f	CTATCATGGCTGGATTGCAG
lzf2060_mDmd-sgRNA3-2r	ATTAAATCTCAAAATAAATG
lzf2063_mDmd-sgRNA4-1f	CTCAATTCAGAATTGGAATGGAT
lzf2064_mDmd-sgRNA4-1r	GTATTATCAGAACACAGGAAAAC
lzf2065_mDmd-sgRNA4-2f	GTGTATGTGTTTGTTTCAGG
lzf2066_mDmd-sgRNA4-2r	CTCATTCTACACAATTTATT
lzf2071_mDmd-sgRNA6-1f	ATATTTCATTCCATCTCTCATTT
lzf2072_mDmd-sgRNA6-1r	TACCTCATGAGCATGAAACTGTT
lzf2073_mDmd-sgRNA6-2f	ACCACTAATTGTATACCACC
lzf2074_mDmd-sgRNA6-2r	CACTTCTTCAACATCATTTG
lzf2077_mDmd-sgRNA7-1f	TAAGATATGCTTAAGAAGAATAT
lzf2078_mDmd-sgRNA7-1r	ATGCTAGCTACCCTGAGACATTC
lzf2079_mDmd-sgRNA7-2f	AATTGCAACTAATAAAATTC
lzf2080_mDmd-sgRNA7-2r	CAAATGAATCTCCTAAATTC
lzf2083_mDmd-sgRNA8-1f	TGAGCAATTGCATTACCTTATAT
lzf2084_mDmd-sgRNA8-1r	GAAAGTGATACTGCACAAGTGGC
lzf2085_mDmd-sgRNA8-2f	TCAGGTGCTTCAAGAAGATC
lzf2086_mDmd-sgRNA8-2r	TAGATACATTTTCATATTGG
lzf2089_mDmd-sgRNA9-1f	GTGGAAGAATGACTGGATTAATC
lzf2090_mDmd-sgRNA9-1r	CAATGAATAAGTGATTTAAGATA
lzf2091_mDmd-sgRNA9-2f	CTATTCTTTACAGGAGATCC
lzf2092_mDmd-sgRNA9-2r	GTTAAATAATAATTGTACAC
lzf2097_mDmd-sgRNA11-1f	ACACAATTAAAGGAGATTGAATT

lzf2098_mDmd-sgRNA11-1r	TAAGAATTAATATCACTTACTTG
lzf2099_mDmd-sgRNA11-2f	ACCTAGACTTAATTTCATTC
lzf3000_mDmd-sgRNA11-2r	GTCCCAACGTTGTGCAAAGT
lzf3003_mDmd-sgRNA12-1f	TCACAGATTTCACAGGCTGTCAC
lzf3004_mDmd-sgRNA12-1r	GCATAATGATTTCTTGGGTAAAT
lzf3005_mDmd-sgRNA12-2f	ACGGTAACTATGGTGACCAC
lzf3006_mDmd-sgRNA12-2r	TTGGGAAATGTGATTCAACT
lzf3009_mDmd-sgRNA13-1f	TCTTCATGGGATATGTATTTTGG
lzf3010_mDmd-sgRNA13-1r	GAAGGAGGAAAACCTTACCTTAC
lzf3011_mDmd-sgRNA13-2f	TGTAGAGGGTGTTAATGCTG
lzf3012_mDmd-sgRNA13-2r	TGGTAGACTGGGTTTTCAAC
lzf3015_mDmd-sgRNA14-1f	GATGAAGTCAACAGATTGTCAGC
lzf3016_mDmd-sgRNA14-1r	CTCTAGCTGCAAATGTAGCTTGT
lzf3017_mDmd-sgRNA14-2f	TCAGCCTCAAATTGAGCAAT
lzf3018_mDmd-sgRNA14-2r	CTTGGTCCTGGGAAGGCTAG
lzf3021_mDmd-sgRNA15-1f	GATATATCATCATGATGAACTAT
lzf3022_mDmd-sgRNA15-1r	CAGGTACTGGAAACTGTCCTAGC
lzf3023_mDmd-sgRNA15-2f	TTCCAGAATCACATAAAAAC
lzf3024_mDmd-sgRNA15-2r	GGCTGAGCTAATTATATAAT
lzf3027_mDmd-sgRNA16-1f	TCAGTCTCTTGAAAATCTGATGC
lzf3028_mDmd-sgRNA16-1r	TCAGACTAAACTGAGCAGAAATC
lzf3029_mDmd-sgRNA16-2f	CAAATCAGATTCGTCTATTG
lzf3030_mDmd-sgRNA16-2r	AGACTGTGTCACTCATATAT
lzf3033_mDmd-sgRNA17-1f	GCAATAATATTAAGAGTATGAAT
lzf3034_mDmd-sgRNA17-1r	TAAATGTTATACTAAGCAGTCGT
lzf3035_mDmd-sgRNA17-2f	TCCAATCAGATTTGACAAGT
lzf3036_mDmd-sgRNA17-2r	TACAGTGTACAGAAGTTATT
lzf3039_mDmd-sgRNA18-1f	CTGAGTGAAGTCAAGTCTGAAGT
lzf3040_mDmd-sgRNA18-1r	CTGAGAATCACAATAAGGGTTTC
lzf3041_mDmd-sgRNA18-2f	CCGGACGTCAAATTGTACAG
lzf3042_mDmd-sgRNA18-2r	TCTATTTTATCTTGAATACT
lzf3045_mDmd-sgRNA19-1f	TGTAGATAGTTGAACAAATGTTT
lzf3046_mDmd-sgRNA19-1r	TTAAAACATTATTTTCATAACAG
lzf3047_mDmd-sgRNA19-2f	ATAACATGGTATATTTCCAT
lzf3048_mDmd-sgRNA19-2r	TACTTCTCATATAATTTCAT
lzf3051_mDmd-sgRNA20-1f	TTCTTGCTCATGGAATATAGCGT
lzf3052_mDmd-sgRNA20-1r	CTTCAGAGTATTGCGCAACCTTC
lzf3053_mDmd-sgRNA20-2f	TAAAGGCTGAAATGAATGAC
lzf3054_mDmd-sgRNA20-2r	ACAAGTTTCCACCTTGAAGT
lzf3057_mDmd-sgRNA21-1f	GCTTATTGGGTGAGGATGACAGT
lzf3058_mDmd-sgRNA21-1r	CACAATTTGTGCAAAGTTGAGTC
lzf3059_mDmd-sgRNA21-2f	CAGCCTATGAAAGTTCTGAG
lzf3060_mDmd-sgRNA21-2r	TGCTGAGCTGGATCTGAGTT

lzf3065_mDmd-sgRNA23-1f	CAGCACACTCTCCATGAAGAAAC
lzf3066_mDmd-sgRNA23-1r	TAGTTTATACATTACCTACCAAG
lzf3067_mDmd-sgRNA23-2f	GTAGTGACGACTGAAGATAT
lzf3068_mDmd-sgRNA23-2r	ATTCTTCAATGTGCAGTAAC
lzf3071_mDmd-sgRNA24-1f	TAAGGTTGATAATTTAGAATTGT
lzf3072_mDmd-sgRNA24-1r	TAATGTTTCAGTAACATTAAAAG
lzf3073_mDmd-sgRNA24-2f	TACTCCCTAGAGAAAGCTAG
lzf3074_mDmd-sgRNA24-2r	GGCTACTTACCCTTGTCGTT
lzf3077_mDmd-sgRNA25-1f	TACTACAAAAGTAATACCTTTGT
lzf3078_mDmd-sgRNA25-1r	TATTGCTGAAAAAATGAAGCCAG
lzf3079_mDmd-sgRNA25-2f	GTGTCCTATAAACCACTTAC
lzf3080_mDmd-sgRNA25-2r	GTCTTACCTTAAGATACCAT
lzf3087_mDmd-sgRNA28-1f	TGACACAATCTGTGGTTACTAAG
lzf3088_mDmd-sgRNA28-1r	AGGTAGCCTAAAAACTATTAGTC
lzf3089_mDmd-sgRNA28-2f	ATGCCATCTTCTTTGCTGTT
lzf3090_mDmd-sgRNA28-2r	GAAATGGAAAGTGACAATAT
lzf3093_mDmd-sgRNA29-1f	CATATTTTCATTTCTAAAAGTCT
lzf3094_mDmd-sgRNA29-1r	TTCTTCAGTAAAATGGCTATCAT
lzf3095_mDmd-sgRNA29-2f	TTCAGGCAACACTGCAAGAT
lzf3096_mDmd-sgRNA29-2r	CTATACCTTGAGCTGTTACT
lzf3099_mDmd-sgRNA30-1f	GATGCACCGTTTAAAGATGTCTG
lzf3100_mDmd-sgRNA30-1r	CAGGACAGCAAGCCAGGCTTTTG
lzf3101_mDmd-sgRNA30-2f	CGGCAGATAAGTGTAGACGT
lzf3102_mDmd-sgRNA30-2r	CATGGTTCATCCAAGGTCAC
lzf3105_mDmd-sgRNA31-1f	ATTCACATTCCCAGCAAGTCTCT
lzf3106_mDmd-sgRNA31-1r	GCCATCTTTATTCATATCTGGAT
lzf3107_mDmd-sgRNA31-2f	TGGTAATTCTGAATGTGTTT
lzf3108_mDmd-sgRNA31-2r	TCTGAAGTTCACTCCACTTG
lzf3111_mDmd-sgRNA32-1f	GAAAGCAGGCTGAAGAGGTCAAC
lzf3112_mDmd-sgRNA32-1r	TGAGTACTCTTTTGGGATCTCTC
lzf3113_mDmd-sgRNA32-2f	GACAAATTGAACCTGCGCTC
lzf3114_mDmd-sgRNA32-2r	CAAAACAAAGCACACAGTAC
lzf3117_mDmd-sgRNA33-1f	TGTAATTCTGGAGATTAATGTTG
lzf3118_mDmd-sgRNA33-1r	TATGAATTTATTATCTATGCTTC
lzf3119_mDmd-sgRNA33-2f	TCCTGTTTACCACGAATTTG
lzf3120_mDmd-sgRNA33-2r	TAGATATTGTAGATGAGAAT
lzf3123_mDmd-sgRNA34-1f	CTTTGCATACTATTGTCCCACTT
lzf3124_mDmd-sgRNA34-1r	GAAAGGAACAAACTCACAGCAAC
lzf3125_mDmd-sgRNA34-2f	CAATAATAAACCTGAGATTG
lzf3126_mDmd-sgRNA34-2r	AACCTAGTCACGACAAATTG
lzf3129_mDmd-sgRNA35-1f	CATTCACGGTTTACTTTTAGTTG
lzf3130_mDmd-sgRNA35-1r	TAAATTGGAAATTAAAATGTCAT
lzf3131_mDmd-sgRNA35-2f	CCTTTTGACCTTTCCATAAT

lzf3132_mDmd-sgRNA35-2r	AGCTGAATAAACAAACAAAG
lzf3137_mDmd-sgRNA36-1f	TGTCTTTAGAATAGGGGAACAAT
lzf3138_mDmd-sgRNA36-1r	ACAGATTATTTTATCAAACAGTT
lzf3139_mDmd-sgRNA36-2f	TGAGAGCAAAGAAATGTTTC
lzf3140_mDmd-sgRNA36-2r	TTCTCCATGTGCAAGTGTGT
lzf4303-mKlkb1-exon3-1f	GGACTTGTCGCAAGAACGTTCTC
lzf4304-mKlkb1-exon3-1r	TTATCTTTCTTGGTGGTCTCGTC
lzf4305-mKlkb1-exon4-1f	CAGTGTTTGATAATTTAGACATG
lzf4306-mKlkb1-exon4-1r	GTTGACTACAGGGAGTTTGCTAC
lzf4311-mKlkb1-exon13-1f	CGGATCACTGCTCCTTCATCTCC
lzf4312-mKlkb1-exon13-1r	TCGTTTTTGAATGAACTGTCTTC
lzf2041_ZF709-IVT-1f	GAAAT TAATACGACTCACTATAGG G GATTCAAGAATCCCGAAGT
lzf2042_ZF709-IVT-1r	TTCTTTTCGGAGACACTCAA TTGAACCTCACACGACTAAA
lzf3141_ZF759- IVT-1r	ATTATCCACAGGTTAACGTC TTGAACCTCACACGACTAAA
lzf3142_ZF769- IVT-1r	GAGAGTTAACTGGCTAGAGT TTGAACCTCACACGACTAAA
lzf3143_ZF774- IVT-1r	TTCAAAGCTGTTACTCGTTC TTGAACCTCACACGACTAAA
lzf3144_ZF780- IVT-1r	GTCTTCTTCTTGTGAATAAT TTGAACCTCACACGACTAAA
lzf3145_ZF789- IVT-1r	CAAACAAAGTGCCCTACTAT TTGAACCTCACACGACTAAA
lzf5034_TnpB-IVT-1f	GAAAT TAATACGACTCACTATAGG G tGGTGGCTGCGGGAATCTC
lzf5035_ IVT-mKlkb1-sg1-1r	TTCTTTAAAGCAGTGTGGCC TTGAACCTCACACGACTAAA
lzf5036_ IVT-mKlkb1-sg2-1r	TTAAAGTTGGACCCTCTCAT TTGAACCTCACACGACTAAA
lzf5037_ IVT-mKlkb1-sg3-1r	TGCGTTTCACCTATGAAGCA TTGAACCTCACACGACTAAA

691

692 **Supplementary Table S3. NGS primers used in this study.**

lzf3762_ZF704-R701-1f	GAATTC NNNNNN GGATCC TCCAGACTGGTCCCCACAAC
lzf3769_ZF704-R707-1r	GACACACTGGTGCCCTCATC
lzf3803_ZF709-R701-1f	GAATTC NNNNNN GGATCC CAACTGCGGAAACTGTAAGT
lzf3832_ZF709-R731-1r	CATGGGTGTTGACCCATTGT
lzf3833_ZF759-R701-1f	GAATTC NNNNNN GGATCC

	GAAAACTATCATGGCTGGAT
lzf4008_mDmd-exon6-2r	TGTACCTGTGACTATGGATAAG
lzf3855_ZF769-R701-1f	GAATTC NNNNNN GGATCC TATTTTGGTTTTCTTTGTAG
lzf3884_ZF769-R731-1r	TTTTCGGCAGTAGTTGTCAT
lzf3885_ZF774-R701-1f	GAATTC NNNNNN GGATCC GGTGATTAAAACCGGACGTC
lzf3643_mDmd-exon33-2r	CTGGTATTCTATTTTATCTT
lzf3904_ZF780-R701-1f	GAATTC NNNNNN GGATCC GCTAGTTTACTTTATGATAT
lzf3647_mDmd-exon43-2r	GTACATTCTATGAAGTTTTT
lzf3924_ZF789-R701-1f	GAATTC NNNNNN GGATCC TCTGGAGATTAATGTTGCCT
lzf3960_ZF789-R738-1r	TTCATGAACATACAGATCAG
lzf3961_ZF790-R701-1f	GAATTC NNNNNN GGATCC CTCCTTCTGTTTTCCCAGGC
lzf3985_ZF790-R726-1r	GAATACTAATACCTGAATCC
lzf3986_ZF759-R701-1f	GAATTC NNNNNN GGATCC GTTATATTTTAACATATAGGTC
lzf4672_ZF1162-R715-1f	GAATTC NNNNNN GGATCC TGTGTTTGTTCAATTCCGCT
lzf4675_ZF1162-R717-1r	GTCCATCATAGTATAAACTT
lzf4676_ZF1163-R718-1f	GAATTC NNNNNN GGATCC GAAGAGCAGTTTATTTGTGT
lzf4661_ZF1163-R705-1r	CTGTAAAATGCACTTGTAGC
lzf4662_ZF1164-R706-1f	GAATTC NNNNNN GGATCC CCTCTCCCGGTCTCTCTTCT
lzf4663_ZF1164-R706-1r	GTTTATAACATAATCTCTGT
lzf5038_ZF1699-R708-1f	GAATTC NNNNNN GGATCC GTGGTGCTTAGAGAAGAGTG
lzf5040_ZF1699-R709-1r	CATCAAGGGACACTCACAGT
lzf5042_ZF1725-R711-1f	GAATTC NNNNNN GGATCC TGAAAAACCTGCAGTTCCAC
lzf5043_ZF1700-R711-1r	GCTCTCTCAGAGCCCGCAAG
lzf5045_ZF1726-R713-1f	GAATTC NNNNNN GGATCC TGAAAAACCTGCAGTTCCAC
lzf5046_ZF1701-R713-1r	GCTCTCTCAGAGCCCGCAAG
lzf5048_ZF1727-R715-1f	GAATTC NNNNNN GGATCC CTTCATGGGTTTCAACTGCG
lzf5049_ZF1702-R715-1r	TGACCCATTGTTCATTTGGC
lzf5051_ZF1729-R719-1f	GAATTC NNNNNN GGATCC CTGCGGAAACTGTAAGTTTG
lzf5052_ZF1704-R719-1r	CATGGGTGTTGACCCATTGT

lzf5054_ZF1730-R721-1f	GAATTC NNNNNN GGATCC CCTCTTTGTATGGATGCATT
lzf5055_ZF1705-R721-1r	TTTTCTGCATCTCTCCAATC

693

Fig.1

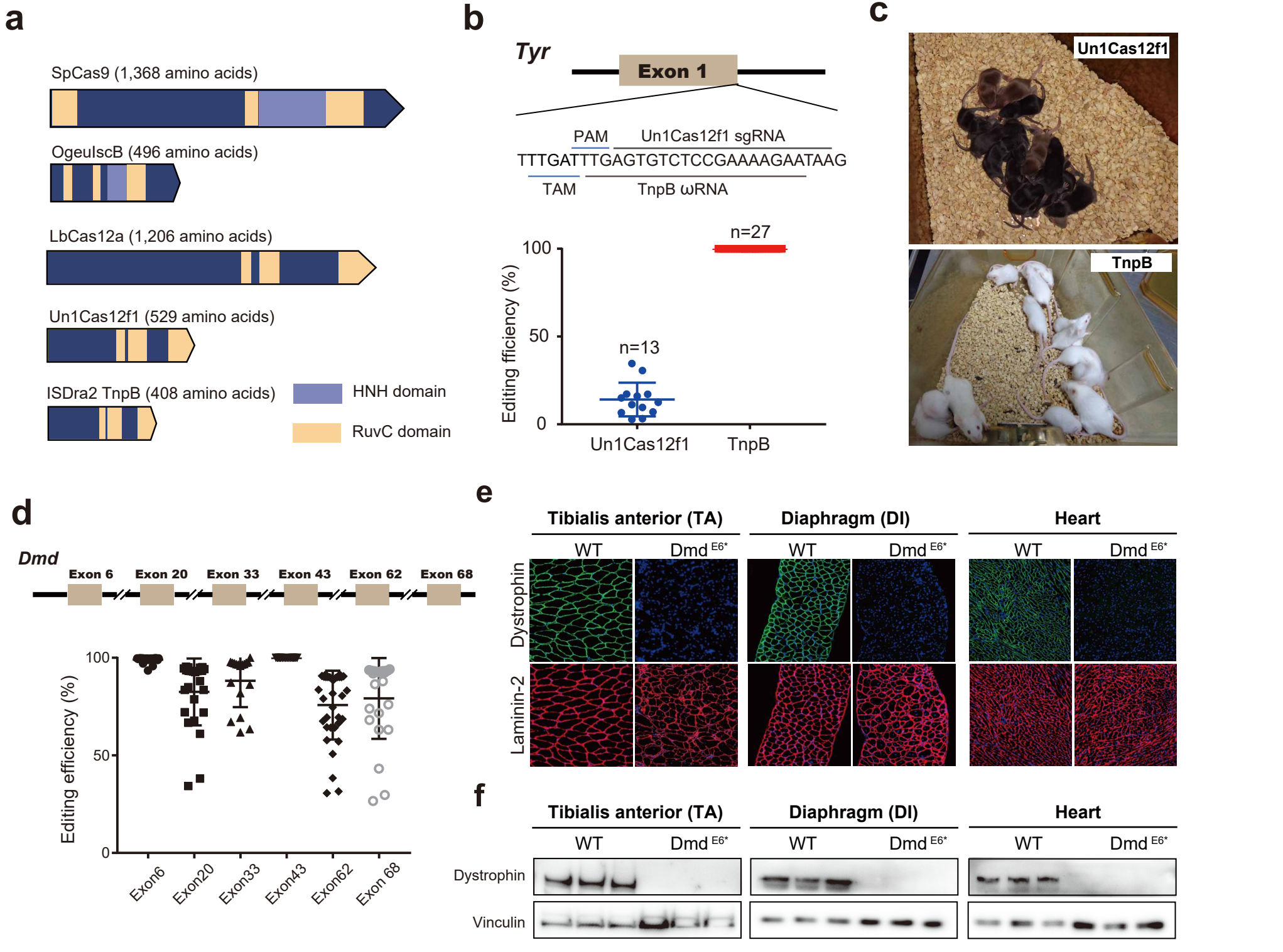
a
SpCas9 (1,368 amino acids)
OgeuIscB (496 amino acids)
LbCas12a (1,206 amino acids)
Un1Cas12f1 (529 amino acids)
ISDra2 TnpB (408 amino acids)
HNH domain
RuvC domain
b
Tyr
Exon 1
PAM
Un1Cas12f1 sgRNA
TTTGATTTGAGTGTCTCCGAAAAGAATAAG
TAM
TnpB ωRNA
Editing fficiency (%)
100
50
0
n=27
n=13
Un1Cas12f1
TnpB
c
Un1Cas12f1
TnpB
d
Dmd
Exon 6
Exon 20
Exon 33
Exon 43
Exon 62
Exon 68
Editing efficiency (%)
100
50
0
Exon6
Exon20
Exon33
Exon43
Exon62
Exon 68
e
Tibialis anterior (TA)
Diaphragm (DI)
Heart
WT
Dmd E6*
Dystrophin
Laminin-2
f
Tibialis anterior (TA)
Diaphragm (DI)
Heart
WT
Dmd E6*
Dystrophin
Vinculin

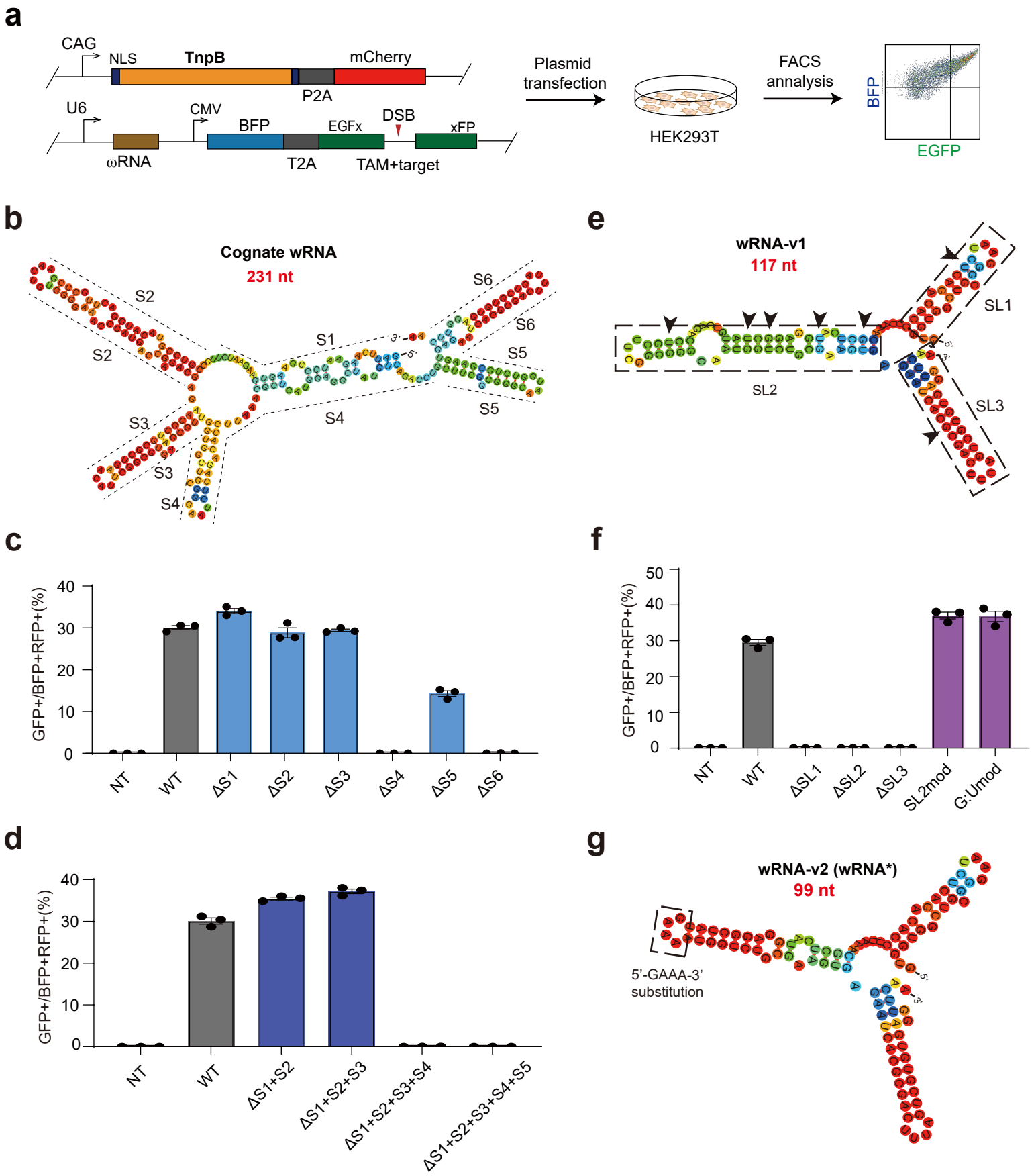

Fig.3

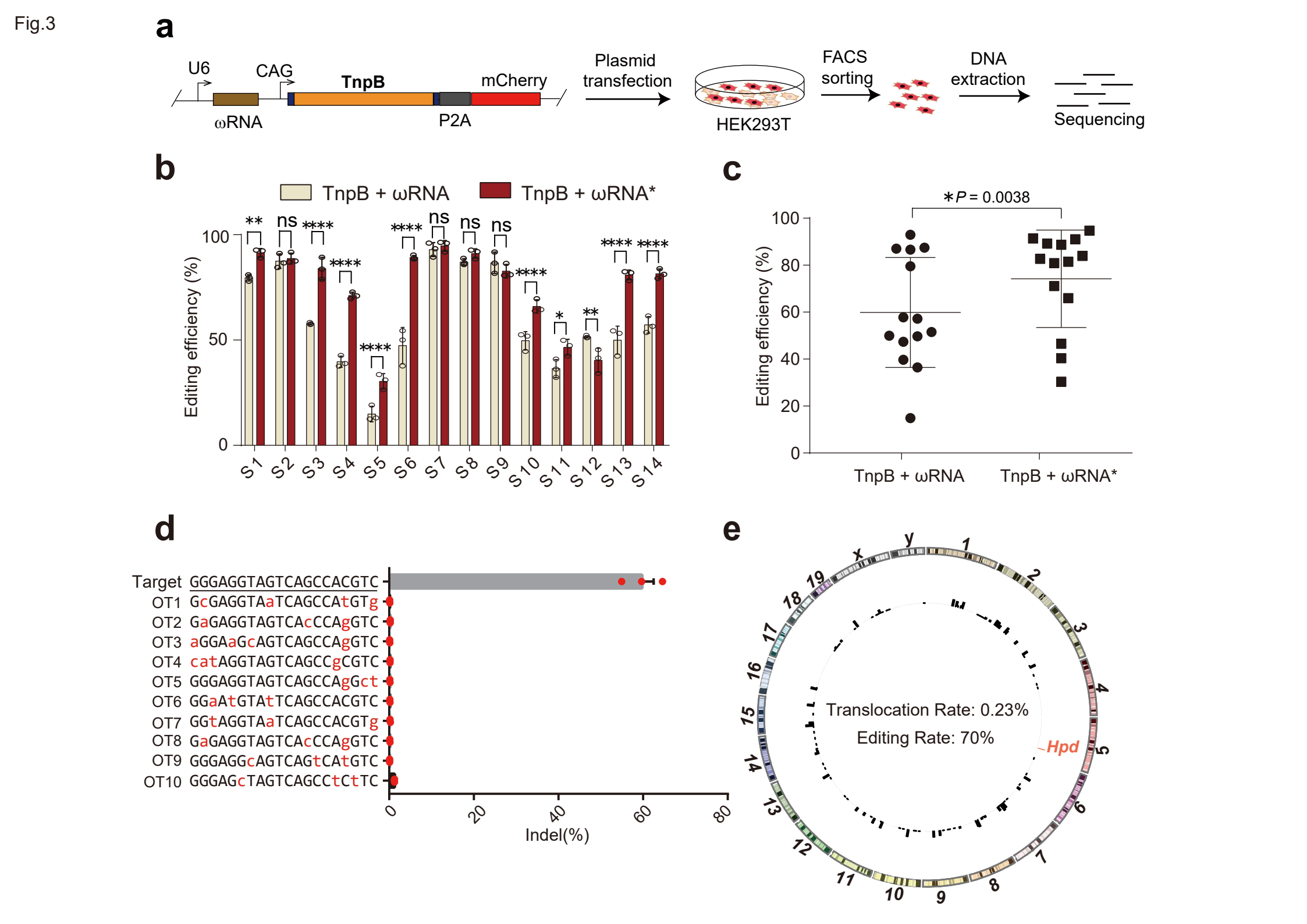
a
U6
CAG
TnpB
mCherry
ωRNA
P2A
Plasmid transfection
HEK293T
FACS sorting
DNA extraction
Sequencing
b
TnpB + ωRNA
TnpB + ωRNA*
Editing efficiency (%)
S1 S2 S3 S4 S5 S6 S7 S8 S9 S10 S11 S12 S13 S14
c
*P = 0.0038
Editing efficiency (%)
TnpB + ωRNA
TnpB + ωRNA*
d
Target GGGAGGTAGTCAGCCACGTC
OT1 GcGAGGTAaTCAGCCAtGTg
OT2 GaGAGGTAGTCAcCCAgGTC
OT3 aGGAaGcAGTCAGCCAgGTC
OT4 catAGGTAGTCAGCCgCGTC
OT5 GGGAGGTAGTCAGCCAgGct
OT6 GGaAtGTAtTCAGCCACGTC
OT7 GGtAGGTAaTCAGCCACGTg
OT8 GaGAGGTAGTCAcCCAgGTC
OT9 GGGAGGcAGTCAGtCAtGTC
OT10 GGGAGcTAGTCAGCCtCtTC
Indel(%)
e
Translocation Rate: 0.23%
Editing Rate: 70%
Hpd

Fig.4

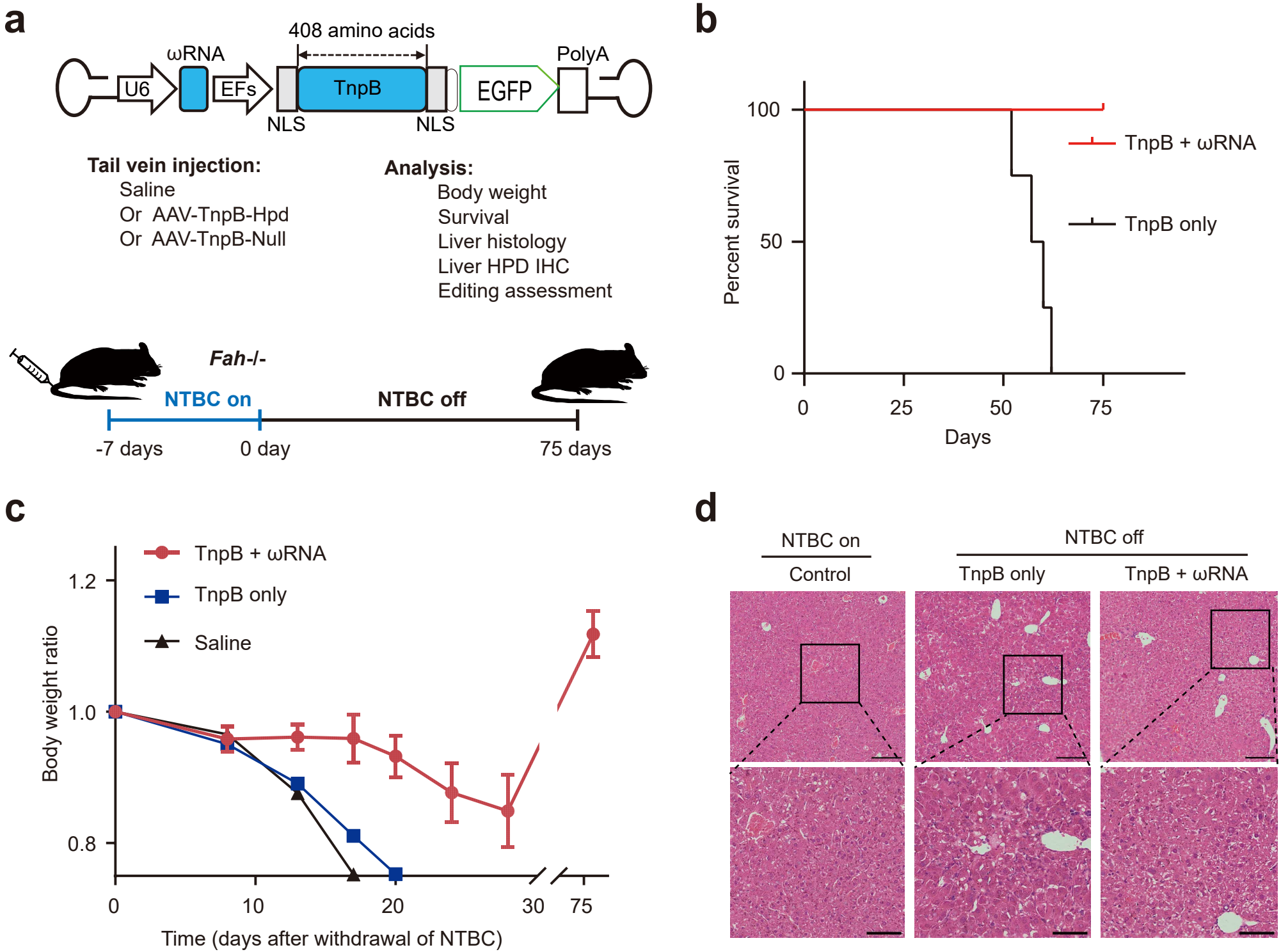
a
408 amino acids
ωRNA
U6
EFs
TnpB
NLS
NLS
EGFP
PolyA
Tail vein injection:
Saline
Or AAV-TnpB-Hpd
Or AAV-TnpB-Null
Analysis:
Body weight
Survival
Liver histology
Liver HPD IHC
Editing assessment
Fah-/-
NTBC on
NTBC off
-7 days
0 day
75 days
b
Percent survival
100
50
0
0
25
50
75
Days
TnpB + ωRNA
TnpB only
c
TnpB + ωRNA
TnpB only
Saline
Body weight ratio
1.2
1.0
0.8
0
10
20
30
75
Time (days after withdrawal of NTBC)
d
NTBC on
NTBC off
Control
TnpB only
TnpB + ωRNA